Bull Math Biol (2017) 79:1325–1359
DOI 10.1007/s11538-017-0287-0

ORIGINAL ARTICLE

Modeling the Fear Effect in Predator–Prey Interactions with Adaptive Avoidance of Predators

Xiaoying Wang[1] · **Xingfu Zou**[1]

Received: 20 July 2016 / Accepted: 3 May 2017 / Published online: 15 May 2017
© Society for Mathematical Biology 2017

Abstract Recent field experiments on vertebrates showed that the mere presence of a predator would cause a dramatic change of prey demography. Fear of predators increases the survival probability of prey, but leads to a cost of prey reproduction. Based on the experimental findings, we propose a predator–prey model with the cost of fear and adaptive avoidance of predators. Mathematical analyses show that the fear effect can interplay with maturation delay between juvenile prey and adult prey in determining the long-term population dynamics. A positive equilibrium may lose stability with an intermediate value of delay and regain stability if the delay is large. Numerical simulations show that both strong adaptation of adult prey and the large cost of fear have destabilizing effect while large population of predators has a stabilizing effect on the predator–prey interactions. Numerical simulations also imply that adult prey demonstrates stronger anti-predator behaviors if the population of predators is larger and shows weaker anti-predator behaviors if the cost of fear is larger.

Keywords Prey–predator interaction · Fear effect · Anti-predator response · Maturation delay · Equilibrium · Stability · Bifurcation

Mathematics Subject Classification 34C23 · 92D25

Research was partially supported by the Natural Sciences and Engineering Research Council of Canada (Grant No. RGPIN-2016-04665).

✉ Xingfu Zou
xzou@uwo.ca

[1] Department of Applied Mathematics, University of Western Ontario, London, ON N6A 5B7, Canada

1 Introduction

Studying the mechanism of predator–prey interaction is a central topic in both ecology and evolutionary biology. Direct killing of prey by predators is obviously easy to observe in the field and hence is the focus of mathematical modeling by far. However, it has been argued by theoretical biologists (Lima 1998, 2009; Creel and Christianson 2008) that indirect effects caused by anti-predator behaviors of prey may play an even more important role in determining prey demography.

Almost all vertebrates demonstrate plastic behaviors in response to stimuli in the surrounding environment. For prey, the fear of predators drives prey to avoid direct predation, which may increase short-term survival probability of prey, but may cause a long-term loss in prey population as a consequence (Cresswell 2011). Such indirect effects exist commonly in species with different life stages in life span, for example, birds. Breeding birds may fly away from nests and leave juvenile birds unprotected and less looked after when adults perceive predation risk (Cresswell 2011). Even the temporary absence of adult birds may lower survival probability of juveniles because juveniles may experience less suitable living conditions provided by adults and face higher risk of predation. In such a scenario, the overall fitness of the bird species may decrease because the fear may lead to a reduction in its reproduction success although its temporal survival probability may increase.

Some recent field experiments supported the aforementioned theoretical arguments about significant effect that such anti-predator behaviors may have. For example, Zanette et al. (2011) conducted a field experiment on song sparrows during a whole breeding season by using electrical fence to eliminate direct predation of both juvenile and adult song sparrows. No direct killing can happen in the experiment; however, broadcast of vocal cues of known predators in the field was employed to mimic predation risk. Two groups of female song sparrows were tested, among which one group was exposed to predator sounds while the other group was not. The authors (Zanette et al. 2011) found that the group of song sparrows exposed to predator vocal cues produced 40% less offspring than the other group because fewer eggs were laid, fewer eggs were successfully hatched, and fewer nestlings survived eventually. Behavioral changes of adult song sparrows when predation risk existed were also observed and documented in Zanette et al. (2011), including less time of adult song sparrows on brood and less feeding to nestlings during breeding period, and these were all believed to be responsible for the total cost of 40% reduction in offspring population. Some correlative experiments on other birds or other vertebrate species (Creel et al. 2007; Sheriff et al. 2009; Wirsing and Ripple 2011) also reported that even though there was no direct killing between predators and prey, the presence of predators did cause a large reduction in prey population due to anti-predator behaviors of prey.

Based on the experiment in Zanette et al. (2011), Wang et al. (2016) studied a predator–prey model with the cost of fear incorporated. The authors found that strong anti-predator behaviors or equivalently the large cost of fear may exclude the existence of periodic solutions and thus eliminate the phenomenon ‘paradox of enrichment.’ In addition, under relatively low cost of fear, periodic solutions still exist arising from either supercritical or subcritical Hopf bifurcation (Wang et al. 2016). In Wang et al. (2016), the age structure of prey is ignored. However, the experiment in Zanette et al.

المنارة للاستشارات

(2011) distinguished the life stages of song sparrows with regard to their behaviors. In addition, the cost of anti-predator defense of adult prey does not only exist in the birth rate of juvenile prey, but also been observed in the survival rates including both natural death rate and predation rate of juveniles. All these evidences suggest the incorporation of age structures into a mathematical model. In fact, the anti-predator behavior of adult prey can be viewed as a plastic trait or strategy which is adaptive to the environment (Yamamichi et al. 2011; Svennungsen et al. 2011). Under selection, adult prey tends to choose a defense level that would increase their survival probability and reduce the reproduction loss, but maximize the individual fitness (Abrams 2000). There have been a few mathematical models that describe such adaptive behaviors of prey. Křivan (2007) studied the trade-off between foraging and predation based on classic Lotka–Volterra model where either prey or predator or both were adaptive to maximize their individual fitness. Peacor et al. (2013) employed a graphical model to study the strength of anti-predator behaviors and conditions when the indirect effects dominate predator–prey interactions by regarding the defense level of prey as an adaptive trait. Takeuchi et al. (2009) studied the conflict between investing time on taking care of juveniles and searching for resources of adult prey in the absence of direct predation, where they assumed that adults adapt their parental care time through learning.

Motivated by the above existing works and the experimental evidence of Zanette et al. (2011) for song sparrows, and as an extension of Wang et al. (2016), in this paper, we formulate, in Sect. 2, a predator–prey model with age structure and allowing adaptive avoidance of predators. The model divides the prey population into a juvenile stage and an adult stage and is naturally represented by a system of delay differential equations (DDEs) with the delay accounting for the maturation time. Adult prey in the model is assumed to adapt defense level in terms of the total growth rate of both juveniles and adults. In Sect. 3, we address the well-posedness of the model with the properly posed initial conditions. In Sect. 4, we analyze the dynamics of the model with either a constant defense level or an adaptive defense level, respectively, with focus on a simplified version of the model. The reason is that for the full model in the general form, analysis becomes much hard and more difficult, as such, we mainly present some numerical simulation results and discuss some biological implications, with focus on the impact of some key model parameters. We conclude the paper by Sect. 5 in which we briefly summarize this work and in the mean time discuss some possible future topics related to this paper.

2 Model Formulation

Based on the experiment in Zanette et al. (2011), there exist different stages of song sparrows, in which song sparrows behave very differently. This naturally suggests use of age-structured model for study of population dynamics of birds. For simplicity, we only consider two stages —a juvenile stage and an adult stage, and follow the standard and frequently used approach (see references Cooke et al. 1999, 2006; Gourley and Kuang 2004; Liu and Beretta 2006; Baer et al. 2006; Wang et al. 2008) to incorporate the two stages of prey into the model. Apparently, there is a maturation delay between juvenile prey and adult prey, which is denoted as τ in our model. Noting that Zanette

المنارة للاستشارات

et al. (2011) reported that juvenile song sparrows cannot live independently and must live under the protection of adult song sparrows to survive, we assume that juvenile birds do not show anti-predator behaviors. In other words, only adult prey is conscious enough to perceive predation risk and is able to void potential attacking by flying away from nests. Such an anti-predator defense of adult prey positively impacts the species survival, but in the mean time results in a cost as well (Creel and Christianson 2008). This is because anti-predator behaviors of adult prey increase the possibility for them to escape from direct killing by predator, but more frequent and defensive flying of adults will consume extra energy and time, which are essential for reproduction. Moreover, too frequent flying of parent birds will leave the juveniles less looked after and less protected, leading to a higher risk of predation. In addition, as documented in Zanette et al. (2011), adult song sparrows feed less to juveniles if they are scared, and this leads to a higher death rate of juvenile song sparrows even in the absence of direct killing.

Taking into consideration the aforementioned facts/observations due to fear effect of adult prey, we can formulate a mathematical model as follows. Let $\alpha \in [0, 1]$ denote the level of anti-predator defense of adult prey, with larger value of α accounting for stronger anti-predation defense and smaller value corresponding to weaker response. Denote the populations of juvenile prey and adult prey by x_1 and x_2, respectively, and the population of predator by y. Adopting the simple mass action predation mechanism and incorporating the effect of the anti-predation response represented by α, the dynamics of x_1 and x_2 can be described by the following differential equations:

$$\begin{cases} \dfrac{\mathrm{d}x_1}{\mathrm{d}t} = b(\alpha, x_2)\, x_2 - (d_0 + d_1\,\alpha)\, x_1 - (s_0 + s_1\,\alpha)\, x_1\, y \\ \qquad\qquad - b(\alpha, x_2(t-\tau))\, x_2(t-\tau) e^{-(d_0 + s_0\, y + (d_1 + s_1\, y)\,\alpha)\,\tau}, \\ \dfrac{\mathrm{d}x_2}{\mathrm{d}t} = b(\alpha, x_2(t-\tau))\, x_2(t-\tau) e^{-(d_0 + s_0\, y + (d_1 + s_1\, y)\,\alpha)\,\tau} \\ \qquad\qquad - d_2\, x_2 - s(\alpha)\, x_2\, y. \end{cases} \tag{1}$$

Here, d_0 is the natural death rate of juveniles, s_0 is the death rate of juveniles due to direct predation, d_1 and s_1 are death rates of juveniles induced by the cost of anti-predator behaviors of adult prey, d_2 is the natural death rate of adult prey. Here in this work, to avoid making things too complicated, we assume that the predator population y is a constant. This corresponds to a scenario that the predator is a generalist which lives on many other species of prey, and this also reflects the environment of the field experiment by Zanette et al. (2011) in which the presence of predators is represented by the strength of vocal cues which can be controlled as a constant level.

In model (1), $b(\alpha, x_2)$ is the birth rate function and $s(\alpha)$ is the predation rate function for adult prey. Both of them depend on the anti-predation behaviors of adult prey and should be decreasing in α, followed by the aforementioned discussions on the fear effect. Typically $b(\alpha, x_2)$ is also decreasing in x_2. To be specific, we choose the following form for $b(\alpha, x_2)$:

$$b(\alpha, x_2) = \begin{cases} (b_0 - b_1\,\alpha)^{\theta_1} e^{(-a\, x_2)}, & \text{if } 0 \le \alpha < \frac{b_0}{b_1}, \\ 0, & \text{if } \frac{b_0}{b_1} \le \alpha \le 1, \end{cases} \tag{2}$$

المنارة للاستشارات

where $0 < b_0 < b_1$ and $\theta_1 \geq 1$. This assumes a threshold b_0/b_1 below which the birth function is of the Ricker type with the maximal birth rate adjusted by $\alpha \in [0, b_0/b_1)$ and above which (extremely fearful case) there is no birth at all. For $s(\alpha)$, for convenience we also choose the following similar form:

$$s(\alpha) = \begin{cases} (s_2 - s_3\,\alpha)^{\theta_2}, & \text{if } 0 \leq \alpha < \frac{s_2}{s_3}, \\ 0, & \text{if } \frac{s_2}{s_3} \leq \alpha \leq 1, \end{cases} \tag{3}$$

where $0 < s_2 < s_3$ and $\theta_2 \geq 1$. Again a threshold s_2/s_3 is assumed above which the adults can fully escape from predation. We point out that depending on the particular species of predator and prey, the two threshold values b_0/b_1 and s_2/s_3 may vary. For convenience of subsequent discussions, we assume, in the rest of the paper, that $s_2/s_3 < b_0/b_1$, accounting for a situation of relatively mild predation.

Because adult prey can perceive predation risk to some extent and *adapt* their behaviors to the change of the surrounding environment (Cresswell 2011), we may consider the anti-predator defense level of the adult prey (i.e., α) to be adaptive. According to Svennungsen et al. (2011), it is reasonable to regard α as a trait, which should evolve toward maximizing the fitness of the prey species (Abrams 2000). For a prey with stage structure, following the idea in Takeuchi et al. (2009), we consider the scenario that adult prey acts adaptively so that the *instant total growth rate of the total species* will be benefitted. With this consideration and following Takeuchi et al. (2009), we adopt the following quantity for the fitness of prey with respect to anti-predator defense level α

$$\begin{aligned} \Phi &= \frac{\mathrm{d}x_1}{\mathrm{d}t} + \frac{\mathrm{d}x_2}{\mathrm{d}t} \\ &= b(\alpha, x_2)\,x_2 - (d_0 + d_1\,\alpha)\,x_1 - (s_0 + s_1\,\alpha)\,y\,x_1 - d_2\,x_2 - s(\alpha)\,x_2\,y. \end{aligned} \tag{4}$$

Then, according to Takeuchi et al. (2009), the evolution of α is governed by

$$\begin{aligned} \frac{\mathrm{d}\alpha}{\mathrm{d}t} &= \gamma(\alpha)\,\frac{\partial \Phi}{\partial \alpha} \\ &= \gamma(\alpha)\left(\frac{\partial b(\alpha, x_2)}{\partial \alpha} x_2 - d_1\,x_1 - s_1\,y\,x_1 - \frac{\mathrm{d}s(\alpha)}{\mathrm{d}\alpha} x_2\,y\right), \end{aligned} \tag{5}$$

where $\gamma(\alpha) = k\,\alpha\,(1-\alpha)$ ensures that the defense level α remains between 0 and 1, provided that $\alpha(0) \in [0, 1]$. Summarizing, as far as the adaptive anti-predator response is concerned, we will consider the following stage-structured predator–prey model with adaptive avoidance of predation and fear effect:

$$\begin{cases} \dfrac{\mathrm{d}x_1}{\mathrm{d}t} = b(\alpha, x_2)\,x_2 - (d_0 + d_1\,\alpha)\,x_1 - (s_0 + s_1\,\alpha)\,x_1\,y \\ \qquad - b(\alpha(t-\tau), x_2(t-\tau))\,x_2(t-\tau)\exp\left(-\displaystyle\int_{t-\tau}^{t} (d_0 + s_0\,y + (d_1 + s_1\,y)\,\alpha(s))\mathrm{d}s\right), \\ \dfrac{\mathrm{d}x_2}{\mathrm{d}t} = b(\alpha(t-\tau), x_2(t-\tau))\,x_2(t-\tau)\exp\left(-\displaystyle\int_{t-\tau}^{t} (d_0 + s_0\,y + (d_1 + s_1\,y)\,\alpha(s))\mathrm{d}s\right) \\ \qquad - d_2\,x_2 - s(\alpha)\,x_2\,y, \\ \dfrac{\mathrm{d}\alpha}{\mathrm{d}t} = k\,\alpha\,(1-\alpha)\left(\dfrac{\partial b(\alpha, x_2)}{\partial \alpha} x_2 - d_1\,x_1 - s_1\,y\,x_1 - \dfrac{\mathrm{d}s(\alpha)}{\mathrm{d}\alpha} x_2\,y\right). \end{cases} \tag{6}$$

المنارة للاستشارات

3 Well-Posedness of the Model

The model (6) should be associated with the nonnegative initial values:

$$x_2(\theta) \geq 0, \quad \alpha(\theta) \in [0, 1] \text{ for } \theta \in [-\tau, 0] \text{ with } x_2(0) > 0. \tag{7}$$

As for the variable x_1, there is also a compatibility issue. To see this, we can integrate the equation for x_1 in (6) to obtain

$$x_1(t) = \int_{t-\tau}^{t} b(\alpha(\eta), x_2(\eta))\, x_2(\eta) \exp\left(-\int_{\eta}^{t} (d_0 + s_0\, y + d_1\, \alpha(u) + s_1\, y\, \alpha(u))\, du\right) \mathrm{d}\eta. \tag{8}$$

At $t = 0$, the above equation gives a constraint on the initial values:

$$x_1(0) = \int_{-\tau}^{0} b(\alpha(\eta), x_2(\eta))\, x_2(\eta) \exp\left(-\int_{\eta}^{0} (d_0 + s_0\, y + d_1\, \alpha(u) + s_1\, y\, \alpha(u))\, du\right) \mathrm{d}\eta. \tag{9}$$

This condition is also biologically reasonable because it simply says that the total juvenile population at $t = 0$ is a result of the newborns during the interval $[-\tau, 0]$ mediated by the death during this period (Kuang and So 1995).

The existence and uniqueness of solutions of (6) can be easily established by the standard method of steps. Now when the initial values are nonnegative and the compatibility condition (9) holds, we can confirm the well-posedness in the sense stated in the following lemma.

Lemma 3.1 *Let $x_2(\theta), \alpha(\theta) \geq 0$ on $-\tau \leq \theta < 0$ and $x_2(0) > 0$, $b_0/b_1 > \alpha(0) > 0$, and assume that $x_1(0)$ satisfies (9). Then, the solution of (6) stays positive and is ultimately bounded.*

Proof Let

$$h(t) = \frac{\partial \Phi}{\partial \alpha}(t) = \frac{\partial b(\alpha(t), x_2(t))}{\partial \alpha}\, x_2(t) - d_1\, x_1(t) - s_1\, y\, x_1(t) - \frac{\mathrm{d}s(\alpha(t))}{\mathrm{d}\alpha(t)}\, y\, x_2(t). \tag{10}$$

Then, $\alpha(t)$ can be expressed as

$$\alpha(t) = \frac{\alpha(0)\, \exp\left(\int_0^t k\, h(\eta)\mathrm{d}\eta\right)}{1 - \alpha(0) + \alpha(0) \exp\left(\int_0^t k\, h(\eta)\mathrm{d}\eta\right)}. \tag{11}$$

Thus, it is clear that $\alpha(t) = 0$ for all $t \geq 0$ if $\alpha(0) = 0$, $\alpha(t) = 1$ for all $t \geq 0$ if $\alpha(0) = 1$, and $0 < \alpha(t) < 1$ for $t \geq 0$ if $0 < \alpha(0) < 1$.

المنارة للاستشارات

Since we assume $x_2(\theta), \alpha(\theta) \geq 0$ on $-\tau \leq \theta < 0$, from equation of x_2 in (6), we obtain

$$\frac{\mathrm{d}x_2(t)}{\mathrm{d}t} \geq -d_2\, x_2 - s(\alpha)\, x_2\, y \geq -\left(d_2 + s_2^2\, y\right) x_2, \quad t \in [0, \tau]. \tag{12}$$

By a comparison argument and from (12), we obtain

$$x_2(t) \geq x_2(0) e^{-(d_2 + s_2^2\, y)t}, \quad t \in [0, \tau] \tag{13}$$

which shows that $x_2(t) > 0$ if $x_2(0) > 0$ for $t \in [0, \tau]$. Repeating the argument, we obtain the positivity in $[\tau, 2\tau]$, $[2\tau, 3\tau]$, ..., and hence for all $t \geq 0$ indeed. The positivity of $x_1(t)$ is just a consequence of combining (8) and the positivity of $x_2(t)$ and $\alpha(t)$.

Next, we show boundedness of solutions of (6). As discussed, we have shown that $\alpha(t)$ is bounded between 0 and 1. Thus, it only remains to show the boundedness of x_1 and x_2. From (6), we have

$$\begin{aligned}
\frac{\mathrm{d}x_1}{\mathrm{d}t} &\leq b(\alpha, x_2)\, x_2 - (d_0 + d_1\, \alpha)\, x_1 - (s_0 + s_1\, \alpha)\, x_1\, y \\
&\leq b_0^{\theta_1}\, e^{-a\, x_2}\, x_2 - (d_0 + s_0\, y)\, x_1 \\
&\leq \frac{b_0^{\theta_1}}{e\, a} - (d_0 + s_0\, y)\, x_1.
\end{aligned}$$

Therefore, we obtain

$$\lim_{t \to \infty} \sup(x_1(t)) \leq \frac{b_0^{\theta_1}}{e\, a\, (d_0 + s_0\, y)}.$$

Furthermore, adding the first two equations of (6) gives

$$\begin{aligned}
\frac{\mathrm{d}(x_1 + x_2)}{\mathrm{d}t} &\leq b(\alpha, x_2)\, x_2 - d_0\, x_1 - d_2\, x_2 \\
&\leq b(\alpha, x_2)\, x_2 - \gamma (x_1 + x_2) \\
&\leq \frac{b_0^{\theta_1}}{e\, a} - \gamma (x_1 + x_2),
\end{aligned}$$

where $\gamma = \min\{d_0, d_2\}$. Thus,

$$\lim_{t \to \infty} \sup(x_1(t) + x_2(t)) \leq \frac{b_0^{\theta_1}}{e\, a\, \gamma}. \tag{14}$$

By (14) and the positivity of x_1 and x_2, we conclude that x_1 and x_2 are ultimately bounded, completing the proof of the lemma. □

المنارة للاستشارات

4 Long-Term Dynamics of the Model

In this section, we investigate the dynamics of the model. We start by looking at two special cases first, in Sects. 4.1 and 4.2, respectively, before considering the full model in Sect. 4.3.

4.1 Model with Constant Defense Level

Before we consider the adaptive defense described by (6), it would be helpful and useful to look at the case when the defense level α is a constant. In this case, the equation of x_2 is decoupled from x_1, and the dynamics of system (1) is completely determined by

$$\frac{\mathrm{d}x_2}{\mathrm{d}t} = b(\alpha, x_2(t-\tau))\, x_2(t-\tau) e^{-(d_0 + s_0\, y + (d_1 + s_1\, y)\,\alpha)\,\tau} - d_2\, x_2 - s(\alpha)\, x_2\, y, \tag{15}$$

where $b(\alpha, x_2), s(\alpha)$ are defined in (2) and (3), respectively. In order to simplify analysis, let $p = d_0 + s_0\, y$, $q = d_1 + s_1\, y$, $\delta_0(\alpha) = p + q\,\alpha$, and $\delta(\alpha) = d_2 + s(\alpha)\, y$.

When the defense level is too strong in the sense that $\alpha \in [b_0/b_1, 1]$, by (2), $b(\alpha, x_2) = 0$, meaning the species is fully devoted to defend predation so that there is no birth at all. Then, (15) becomes

$$\frac{\mathrm{d}x_2}{\mathrm{d}t} = -d_2\, x_2 - s(\alpha)\, x_2\, y, \tag{16}$$

implying that $x_2(t)$ dies out exponentially. Accordingly, by the first equation in (6), $x_1(t)$ also approaches zero.

Next, consider the case of mild defense, that is, $\alpha \in [0, b_0/b_1)$. Then, plugging in the birth function given in (2) into (15) leads to

$$\frac{\mathrm{d}x_2}{\mathrm{d}t} = (b_0 - b_1\alpha)^{\theta_1} e^{-\delta_0(\alpha)\tau} e^{-a x_2(t-\tau)} x_2(t-\tau) - \delta(\alpha) x_2. \tag{17}$$

This is in the form of the well-known Nicholson blowfliy equation which has been extensively studied in the literature, see, e.g., Cooke et al. (1999), Faria (2006), Győri and Trofimchuk (2002), Shu et al. (2013), Wei and Li (2005), and the references therein. In terms of the so-called basic reproduction number

$$\mathcal{R}_0 = \frac{(b_0 - b_1\alpha)^{\theta_1}\, e^{-\delta_0(\alpha)\tau}}{\delta(\alpha)}, \tag{18}$$

the main results about (17) related to the topics of this paper are summarized as follows:

(C1) If $\mathcal{R}_0 \le 1$, then the trivial equilibrium $x_2 = 0$ is globally asymptotically stable.
(C2) If $\mathcal{R}_0 > 1$, then the trivial equilibrium becomes unstable and there exists a unique positive equilibrium given by $x_2^+ = \frac{1}{a} \ln \mathcal{R}_0$. In this case, for any fixed $\tau > 0$,

المنارة للاستشارات

(C2-i) either x_2^+ is locally asymptotically stable
(C2-ii) or x_2^+ is unstable, but there is a locally asymptotically stable periodic solution $x_{2p}(t)$ that is a sustained oscillation about x_2^+.

Since in both (C2-i) and (C2-ii), $x_2^+ = \frac{1}{a}\ln \mathcal{R}_0$ represents the average persistence level of the population, it is interesting and significant to explore at what value of $\alpha \in [0, b_0/b_1)$, $\mathcal{R}_0 = \mathcal{R}_0(\alpha)$ will be maximized. Note that $s(\alpha) = 0$ for $\alpha \in [s_2/s_3, 1]$, and hence, $\mathcal{R}_0(\alpha)$ is deceasing in $[s_2/s_3, 1]$. Thus, $\mathcal{R}_0$ should be maximized in the interval $[0, s_2/s_3]$. The following theorem gives an answer to the problem when $\theta_1 = 1 = \theta_2$.

Theorem 4.1 *Let $\theta_1 = 1 = \theta_2$. Then, $\mathcal{R}_0$ is maximized at $\alpha = 0$ if*

$$\exp\left(\frac{q\,\tau\,s_2}{s_3}\right) > \frac{(d_2 + s_2\,y)\,(b_0\,s_3 - b_1\,s_2)}{b_0\,d_2\,s_3}, \tag{19}$$

and it is maximized at $\alpha = s_2/s_3$ if (19) is reversed.

Proof For $0 \le \alpha \le s_2/s_3$, we have

$$\frac{\mathrm{d}\mathcal{R}_0}{\mathrm{d}\alpha} = \frac{-e^{-p\tau}e^{-q\tau\alpha}}{(d_2 + ys_2 - ys_3\alpha)^2}\left[a_1\,\alpha^2 + a_2\,\alpha + a_3\right] \tag{20}$$

where

$$\begin{aligned} a_1 &= q\,\tau\,b_1\,y\,s_3,\ a_2 = -q\,\tau\,(b_1\,d_2 + b_1\,y\,s_2 + s_3\,y\,b_0)\,, \\ a_3 &= q\,\tau\,b_0\,(d_2 + s_2\,y) + b_1\,d_2 - y\,(b_0\,s_3 - b_1\,s_2)\,. \end{aligned} \tag{21}$$

Let

$$\begin{aligned} \Delta = a_2^2 - 4a_1a_3 = q\tau\,(s_3yb_0 - b_1d_2 - b_1ys_2)\,(q\tau b_0ys_3 + 4b_1s_3y \\ -q\tau b_1ys_2 - q\tau b_1d_2)\,. \end{aligned} \tag{22}$$

If $a_3 > 0$ and $\Delta < 0$, (20) has no real root and $\mathcal{R}_0$ is maximized either at $\alpha = 0$ or $\alpha = s_2/s_3$. If $a_3 > 0$ and $\Delta > 0$, then (20) has two distinct positive roots

$$\bar{\alpha}_1 = \frac{-a_2 - \sqrt{\Delta}}{2\,a_1},\quad \bar{\alpha}_2 = \frac{-a_2 + \sqrt{\Delta}}{2\,a_1},$$

where $\bar{\alpha}_2 > s_2/s_3$ and hence should be excluded. Direct calculations show that $\alpha = \bar{\alpha}_1$ is the local minimum point of R_0, and hence, $\mathcal{R}_0$ is maximized either at $\alpha = 0$ or $\alpha = s_2/s_3$. If $a_3 < 0$, then (20) has a single positive root $\bar{\alpha}_2$ which is in $[s_2/s_3, 1]$. Summarizing in the interval $0 \le \alpha \le s_2/s_3$, $\mathcal{R}_0$ can only be maximized either at $\alpha = 0$ or at $\alpha = s_2/s_3$. Evaluation of $\mathcal{R}_0(0)$ and $\mathcal{R}_0(s_2/s_3)$ leads to the conclusion of the theorem, and the proof is completed. □

For other values of θ_1 and θ_2, one may also do similar things, but it typically becomes more difficult for analytic results. However, one can always explore numerically to gain

المنارة للاستشارات

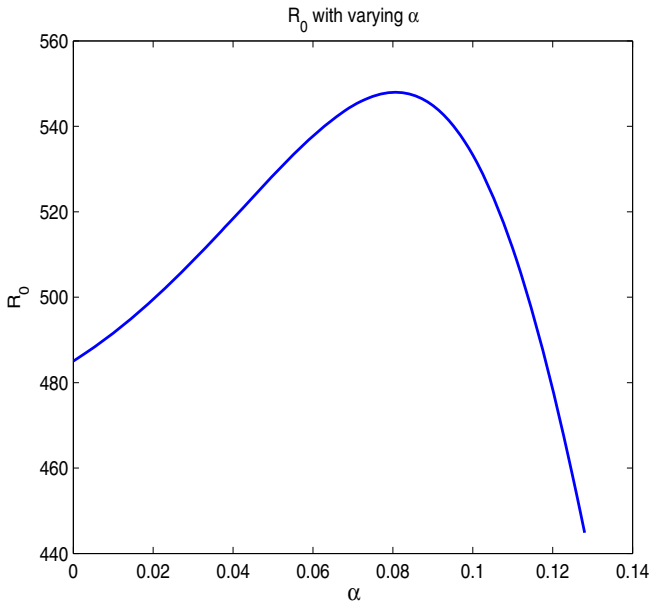

Fig. 1 If $\theta_1 = \theta_2 = 2$, optimal defense level α exists in interval $[0, s_2/s_3]$. Other parameters are $b_0 = 9.4609, b_1 = 13.2741, p = 0.0856, q = 3.0554, d_2 = 0.0467, s_2 = 0.2009, s_3 = 1.5685, y = 2.6194, \tau = 2.2335$

useful information on this topic. For example, for $\theta_1 = \theta_2 = 2$ and with parameters given, numerical results show that an optimal defense level α may exist in the interval $0 < \alpha < s_2/s_3$, as demonstrated in Fig. 1.

4.2 Model with Adaptive Defense Level—A Special Case: $d_1 = 0,\ \ s_1 = 0$

In this subsection, we first consider a special case where the anti-predation response of adult prey has no impact on the death and predation of juveniles. This is reflected by assuming $d_1 = 0,\ s_1 = 0$ in (6), leading to the following simplified version of the model:

$$\begin{aligned}
\frac{\mathrm{d}x_1}{\mathrm{d}t} &= b(\alpha,\ x_2)\, x_2 - (s_0\, y + d_0)\, x_1 \\
&\quad - b(\alpha(t-\tau), x_2(t-\tau))\, x_2(t-\tau) e^{-(d_0 + s_0\, y)\tau}, \\
\frac{\mathrm{d}x_2}{\mathrm{d}t} &= b(\alpha(t-\tau), x_2(t-\tau))\, x_2(t-\tau) e^{-(d_0 + s_0\, y)\,\tau} - d_2\, x_2 - s(\alpha)\, x_2\, y, \\
\frac{\mathrm{d}\alpha}{\mathrm{d}t} &= k\,\alpha\,(1-\alpha)\left(\frac{\partial b(\alpha, x_2)}{\partial \alpha}\, x_2 - \frac{\mathrm{d}s(\alpha)}{\mathrm{d}\alpha}\, x_2\, y\right),
\end{aligned} \tag{23}$$

where $b(\alpha, x_2)$ and $s(\alpha)$ are the same functions defined in (2) and (3), respectively. To be more concrete, we will choose $\theta_1 = \theta_2 = 2$ in this subsection.

المنارة للاستشارات

Notice that the equations for $x_2'(t)$ and $\alpha'(t)$ in (23) are decoupled from the equation for $x_1'(t)$. Therefore, we only need, in the rest of this subsection, to study subsystem

$$\begin{aligned}\frac{\mathrm{d}x_2}{\mathrm{d}t} &= b(\alpha(t-\tau), x_2(t-\tau))\, x_2(t-\tau) e^{-p\,\tau} - d_2\, x_2 - s(\alpha)\, x_2\, y,\\ \frac{\mathrm{d}\alpha}{\mathrm{d}t} &= k\,\alpha\,(1-\alpha)\left(\frac{\partial b(\alpha, x_2)}{\partial \alpha}\, x_2 - \frac{\mathrm{d}s(\alpha)}{\mathrm{d}\alpha}\, x_2\, y\right),\end{aligned} \tag{24}$$

where $p = d_0 + s_0\, y$.

4.2.1 Model Without Delay

We first analyze the special case of (24) when the delay is absent, i.e., $\tau = 0$. In this special case, system (24) is reduced to the following ODE system

$$\begin{aligned}\frac{\mathrm{d}x_2}{\mathrm{d}t} &= b(\alpha, x_2)\, x_2 - d_2\, x_2 - s(\alpha)\, x_2\, y,\\ \frac{\mathrm{d}\alpha}{\mathrm{d}t} &= k\,\alpha\,(1-\alpha)\left(\frac{\partial b(\alpha, x_2)}{\partial \alpha}\, x_2 - \frac{\mathrm{d}s(\alpha)}{\mathrm{d}\alpha}\, x_2\, y\right).\end{aligned} \tag{25}$$

First, we note that there is a continuum of extinction equilibria $(0, \alpha)$, $\alpha \in [0, 1]$. Obviously none of these can be stable due to the continuum property, but it is possible that some of them may attract some solutions. By (2) and (3), we need to investigate (25) in a piecewise fashion, as proceeded.

For $\alpha \in [b_0/b, 1]$, (25) reduces to

$$\begin{aligned}\frac{\mathrm{d}x_2}{\mathrm{d}t} &= -d_2\, x_2,\\ \frac{\mathrm{d}\alpha}{\mathrm{d}t} &= 0.\end{aligned} \tag{26}$$

Thus, if $\alpha(0) = \alpha_0 \in [b_0/b, 1]$ and $x_2(0) > 0$, then $\alpha(t)$ remain constant α_0 and $x_2(t)$ decay to 0 exponentially.

For $\alpha \in [s_2/s_3, b_0/b_1)$, (25) becomes

$$\begin{aligned}\frac{\mathrm{d}x_2}{\mathrm{d}t} &= (b_0 - b_1\,\alpha)^2\, e^{-a\,x_2}\, x_2 - d_2\, x_2 =: d_2\left[\mathcal{R}_1(\alpha) e^{-a x_2} - 1\right] x_2\\ \frac{\mathrm{d}\alpha}{\mathrm{d}t} &= -2\,k\,\alpha\,(1-\alpha)\, b_1\,(b_0 - b_1\,\alpha)\, e^{-a\,x_2}\, x_2 =: h_1(\alpha) e^{-a x_2} x_2,\end{aligned} \tag{27}$$

where $\mathcal{R}_1(\alpha) = (b_0 - b_1\,\alpha)^2/d_2$ is the adaptive (w.r.t α) reproduction number and $h_1(\alpha) = -2\,k\,\alpha\,(1-\alpha)\, b_1\,(b_0 - b_1\,\alpha)$. Obviously $h_1(\alpha) < 0$ for $\alpha \in [s_2/s_3, b_0/b_1)$, meaning that $\alpha'(t) < 0$. Thus, if $\alpha(0) = \alpha_0 \in [s_2/s_3, b_0/b_1)$, then $\alpha(t)$ remains decreasing for all $t > 0$ as long as $\alpha(t)$ remains in $[s_2/s_3, b_0/b_1)$. Note that $\mathcal{R}_1(\alpha)$ is decreasing. Thus, if $\mathcal{R}_1(s_2/s_3) < 1$, then $\mathcal{R}_1(\alpha) e^{-a x_2} - 1 < \mathcal{R}_1(s_2/s_3) - 1 < 0$, meaning that $x_2(t)$ remains decreasing for all $t > 0$. But if $\mathcal{R}_1(s_2/s_3) > 1$, then

المنارة للاستشارات

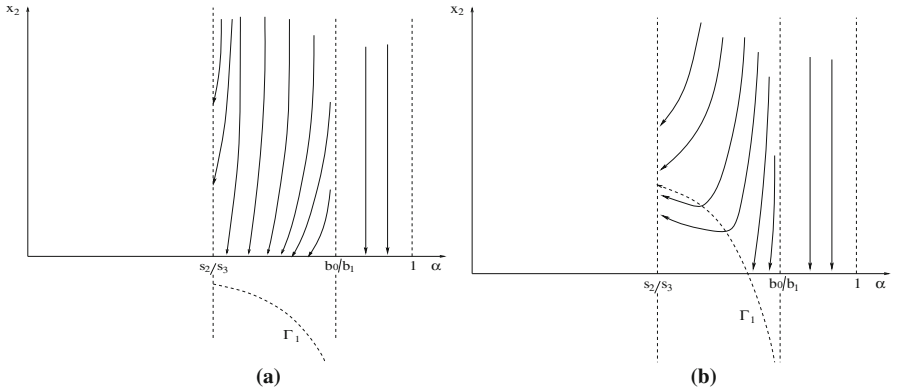

Fig. 2 Dynamics within $\alpha \in [s_2/s_3, 1]$. **a** $\mathcal{R}_1(s_2/s_3) < 1$ and **b** $\mathcal{R}_1(s_2/s_3) > 1$

the curve $\Gamma_1 : \ x_2 = \frac{1}{a} \ln \mathcal{R}_1(\alpha)$ has a portion in the region $\Omega_1 = \{(\alpha, x_2) : \alpha \in [s_2/s_3, b_0/b_1), \ x_2 > 0\}$, above which $x_2'(t) < 0$ and below which $x_2'(t) > 0$.

The phase portraits of the model on the stripe $\alpha \in (s_2/s_3, 1]$ are demonstrated in Fig. 2. Note that there is no equilibrium that has positive x_2 component in this region.

For $\alpha \in [0, s_2/s_3)$, (25) is represented by

$$\begin{aligned} \frac{\mathrm{d}x_2}{\mathrm{d}t} &= \left[d_2 + (s_2 - s_3\alpha)^2 y\right]\left[\mathcal{R}_2(\alpha)e^{-ax_2} - 1\right] x_2, \\ \frac{\mathrm{d}\alpha}{\mathrm{d}t} &= 2\,k\,\alpha\,(1-\alpha)s_3\,(s_2 - s_3\,\alpha)\,y e^{-a\,x_2}\left[e^{ax_2} - W(\alpha)\right] x_2, \end{aligned} \tag{28}$$

where the adaptive (w.r.t. α) reproduction number $\mathcal{R}_2(\alpha)$ and the other auxiliary function $W(\alpha)$ are given by

$$\mathcal{R}_2(\alpha) = \frac{(b_0 - b_1\alpha)^2}{d_2 + (s_2 - s_3\alpha)^2\, y}, \quad W(\alpha) = \frac{b_1(b_0 - b_1\alpha)}{s_3(s_2 - s_3\alpha)y}. \tag{29}$$

The dynamics of (25) in $\Omega_2 = \{(\alpha, x_2) : \alpha \in [0, s_2/s_3), \ x_2 > 0\}$ is determined by the positions of the two nullclines $\Gamma_2 : \ x_2 = \frac{1}{a} \ln \mathcal{R}_2(\alpha)$ and $\Gamma_3 : \ x_2 = \frac{1}{a} \ln W(\alpha)$.

Firstly, under the assumption of $s_2/s_3 < b_0/b_1$, one can easily verify that $W(\alpha)$ is increasing on $[0, s_2/s_3)$ with $W(\alpha) \to \infty$ as $\alpha \to (s_2/s_3)^+$. For $\mathcal{R}_2(\alpha)$, one can calculate $\mathcal{R}_2'(\alpha)$ to obtain

$$\mathcal{R}_2'(\alpha) = \frac{2(b_0 - b_1\alpha)}{[d_2 + (s_2 - s_3\alpha)^2 y]^2}\left[-b_1 d_2 + y s_2(b_0 s_3 - b_1 s_2) - y s_3(b_0 s_3 - b_1 s_2)\alpha\right].$$

Thus, $\mathcal{R}_2(\alpha)$ is decreasing in $[0, s_2/s_3)$ if $y s_2(b_0 s_3 - b_1 s_2) < b_1 d_2$ which is equivalent to $W(0) > \mathcal{R}_2(0)$, and it has a unique maximum at $\alpha^* = [y s_2(b_0 s_3 - b_1 s_2) - b_1 d_2]/[y s_2(b_0 s_3 - b_1 s_2)]$ if $W(0) < \mathcal{R}_2(0)$. These properties of $\mathcal{R}_2(\alpha)$ pass to $\ln \mathcal{R}_2(\alpha)$. Based on this observation, we can distinguish two cases: (A) $W(0) > \mathcal{R}_2(0)$ and (B) $W(0) < \mathcal{R}_2(0)$. In case (A), Γ_2 and Γ_3 do not intersect at all in $(0, s_2/s_3)$, and

المنارة للاستشارات

therefore, (B) is a *necessary condition* for the model to have an interior equilibrium. In case (B), Γ_2 and Γ_3 have precisely one intersect Q, but it can be above or below the α-axis, distinguishing existence and nonexistence of a positive equilibrium. We explore sufficient conditions for the existence in the sequel.

Let $\psi = e^{-ax_2}$. By $W(\alpha) - 1/\psi = 0$, we see that a positive equilibrium $E(\bar{x}_2,\ \bar{\alpha})$ must satisfy

$$\bar{x}_2 = \frac{-1}{a}\ \ln(\psi), \quad \bar{\alpha} = \frac{b_0\, b_1\, \psi - s_2\, s_3\, y}{b_1^2\, \psi - s_3^2\, y} =: H(\psi) \tag{30}$$

where, by plugging the formula for $\bar{\alpha}$ in (30) into $\mathcal{R}_2(\alpha) - 1/\psi = 0$ and solving the resulting quadratic equation, ψ is given by

$$\psi = \frac{d_2\, s_3^2\, y}{y\,(b_0\, s_3 - b_1\, s_2)^2 + b_1^2\, d_2}. \tag{31}$$

Noting that with the assumption of $s_2/s_3 < b_0/b_1$, $H(\psi)$ is decreasing in $\psi \in (0, 1)$ with $H(0) = s_2/s_s$, which automatically ensures that $\bar{\alpha} < s_2/s_3$. Now the other requirement of $\bar{\alpha} > 0$ leads to another constraint for ψ : $\psi < s_2 s_3 y/b_0 b_1$, which is obtained by solving $H(\psi) = 0$ for ψ. Thus, we need to impose constrain for (31) to be in the interval $(0, \psi_0)$ where

$$\psi_0 = \min\left\{\frac{s_2\, s_3\, y}{b_0\, b_1},\ 1\right\}. \tag{32}$$

It is easy to verify that $\psi < s_2 s_3 y/b_0 b_1$ is equivalent to $W(0) < \mathcal{R}_2(0)$ which is explicitly expressed as

$$y > \frac{d_2\, b_1}{s_2\,(b_0\, s_3 - b_1\, s_2)}. \tag{33}$$

Thus, we have obtained the following theorem about the existence of an interior equilibrium.

Theorem 4.2 *Assume that* (33) *is satisfied (necessary condition). Then, a unique interior equilibrium* $E(\bar{x}_2, \bar{\alpha})$ *of* (25) *exists if either (i)* $W(0) \geq 1$, *or (ii)* $W(0) < 1$ *and* $\psi < 1$.

In addition to the interior equilibrium under the condition of Theorem 4.2, there is also a no-fear equilibrium $E_s = (\bar{x}_{20}, 0)$ provided that $\mathcal{R}_2(0) > 1$, where $\bar{x}_{20} = \frac{1}{a} \ln \mathcal{R}_2(0)$. The stability of E_s is determined by the two eigenvalues of the linearization at E_s which are explicitly obtained as

$$\lambda_1 = -a\, \bar{x}_{20}\, \left(d_2 + s_2^2\, y\right) < 0, \quad \lambda_2 = -2\, k\, \bar{x}_{20}\, \left(\frac{\left(d_2 + s_2^2\, y\right)\, b_1 - s_2\, s_3\, y\, b_0}{b_0}\right). \tag{34}$$

Thus, $E_s(\bar{x}_{20}, 0)$ is locally asymptotically stable if and only if

$$\lambda_2 < 0 \Leftrightarrow y < \frac{d_2\, b_1}{s_2\,(b_0\, s_3 - b_1\, s_2)}, \tag{35}$$

المنارة للاستشارات

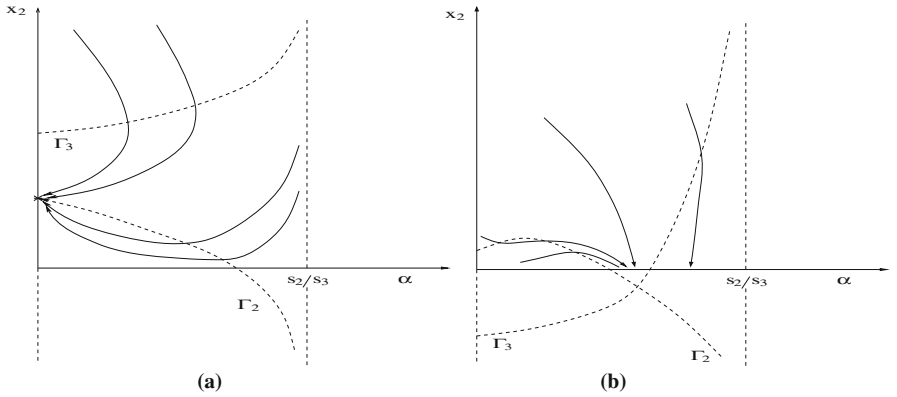

Fig. 3 Dynamics within $\alpha \in [0, s_2/s_3)$ for the case $\mathcal{R}_2(0) > 1$ in the absence of interior equilibrium. **a** $1 < \mathcal{R}_2(0) < W(0)$ and **b** $\mathcal{R}_2(0) > 1 > W(0)$ with intercept *below* α-axis

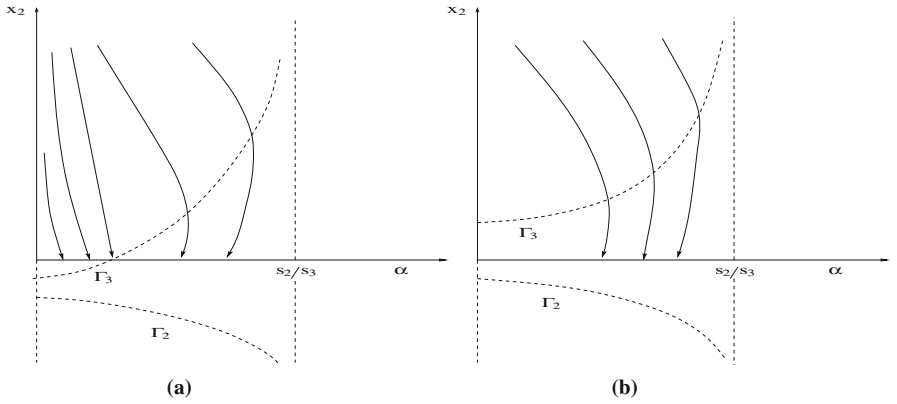

Fig. 4 Dynamics within $\alpha \in [0, s_2/s_3)$ for the case $\mathcal{R}_2(0) < 1$. **a** $W(0) < 1$ and **b** $W(0) > 1$

which is equivalent to $W(0) > \mathcal{R}_2(0)$. This leads to the following theorem.

Theorem 4.3 *Assume that* $\mathcal{R}_2(0) > 1$. *Then,* E_s *is asymptotically stable if and only if* (35) *holds.*

See Fig. 3a for an illustration of the dynamics for this case.

When $\mathcal{R}_2(0) < 1$, E_s disappears and there is no equilibrium with positive x_2 value. In this case, solutions approach to different points on the α-axis, depending on the initial values. See Fig. 4a, b for an illustration of the solution behaviors.

As for the stability of the unique interior equilibrium $E(\bar{x}_2, \bar{\alpha})$ under the condition of Theorem 4.2, we can also calculate the two eigenvalues of the linearization at $E(\bar{x}_2, \bar{\alpha})$ to obtain the two eigenvalues as follows:

$$\lambda_1 = \frac{-a\bar{x}_2 d_2 \left[y\,(b_0\,s_3 - b_1\,s_2)^2 + b_1^2\,d_2\right]}{y\,(b_0\,s_3 - b_1\,s_2)^2},$$

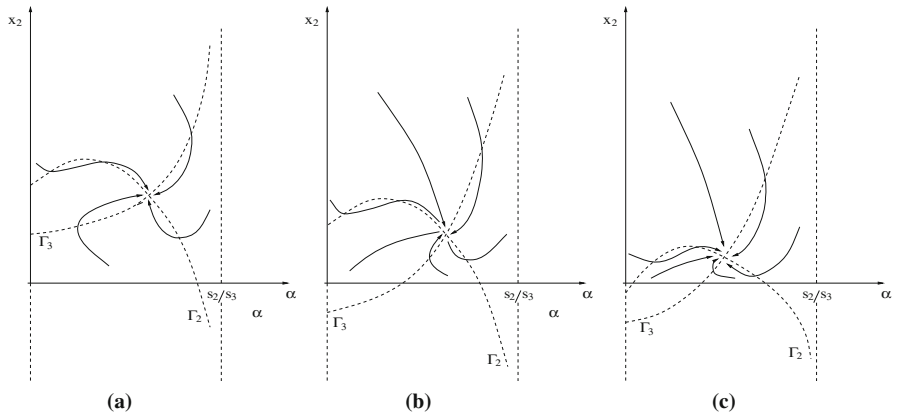

Fig. 5 Dynamics within $\alpha \in [0, s_2/s_3)$ in the presence of a positive equilibrium. **a** $\mathcal{R}_2(0) > W(0) > 1$, **b** $W(0) < 1 < \mathcal{R}_2(0)$ with intersect *above* α-axis, **c** $W(0) < \mathcal{R}_2(0) < 1$ with intercept is *above* α-axis

$$\lambda_2 = \frac{2a\bar{x}_2 k\left[(b_0 s_3 - b_1 s_2)(s_2 - s_3)\, y - b_1 d_2\right]\left[s_2\, y\,(b_0 s_3 - b_1 s_2) - b_1 d_2\right]}{a\left[y\,(b_0 s_3 - b_1 s_2)^2 + b_1^2 d_2\right]}. \tag{36}$$

Obviously $\lambda_1 < 0$, and $\lambda_2 < 0$ if and only if (33) holds. Therefore, we have shown that the positive equilibrium $E(\bar{x}_2, \bar{\alpha})$ is asymptotically stable, as long as it exists, as stated in the following theorem.

Theorem 4.4 *Under the conditions of Theorem 4.2, a unique interior equilibrium $E(\bar{x}_2, \bar{\alpha})$ not only exists, but also is asymptotically stable (Fig. 5).*

4.2.2 Equilibria of System (24) When $\tau > 0$

When $\tau > 0$, similar to (25), (24) also has concrete forms for $\alpha \in [b_0/b_1, 1]$, $\alpha \in [s_2/s_3, b_0/b_1)$ and $\alpha \in [0, s_2/s_3)$, respectively. For $\alpha \in [b_0/b_1, 1]$, (24) still reduces to (26); for $\alpha \in [s_2/s_3, b_0/b_1)$, (24) becomes

$$\begin{aligned}
\frac{\mathrm{d}x_2}{\mathrm{d}t} &= (b_0 - b_1\,\alpha(t-\tau))^2\, e^{-a\,x_2(t-\tau)}\, x_2(t-\tau) - d_2\, x_2 \\
&=: d_2\left[\hat{\mathcal{R}}_1(\alpha(t-\tau), \tau) e^{-a x_2(t-\tau)} x_2(t-\tau) - x_2(t)\right] \\
\frac{\mathrm{d}\alpha}{\mathrm{d}t} &= -2\,k\,\alpha\,(1-\alpha)\,b_1\,(b_0 - b_1\,\alpha)\, e^{-a\,x_2(t)}\, x_2(t) =: h_1(\alpha) e^{-a x_2(t)} x_2(t),
\end{aligned} \tag{37}$$

where $\hat{\mathcal{R}}_1(\alpha, \tau) = \mathcal{R}_1(\alpha) e^{-p\tau}$ with $\mathcal{R}_1(\alpha)$ and $h_1(\alpha)$ being the same as in (27), while for $\alpha \in [0, s_2/s_3)$, the model reduces to

$$\frac{\mathrm{d}x_2}{\mathrm{d}t} = \left[d_2 + (s_2 - s_3\alpha(t))^2 y\right]\left[\hat{\mathcal{R}}_3(\alpha(t), \alpha(t-\tau), \tau) e^{-a x_2(t-\tau)} x_2(t-\tau) - x_2(t)\right],$$

المنارة للاستشارات

$$\frac{d\alpha}{dt} = 2\,k\,\alpha\,(1-\alpha)s_3\,(s_2 - s_3\,\alpha)ye^{-a\,x_2(t)}\left[e^{ax_2(t)} - W(\alpha)\right]x_2(t), \tag{38}$$

where $W(\alpha)$ is as in (29) and

$$\hat{\mathcal{R}}_3(\alpha,\beta,\tau) = \frac{(b_0 - b_1\beta)^2 e^{-p\tau}}{d_2 + (s_2 - s_3\alpha)^2\,y}.$$

Let $\hat{\mathcal{R}}_2(\alpha,\tau) := \hat{\mathcal{R}}_3(\alpha,\alpha,\tau) = \mathcal{R}_2(\alpha)e^{-p\tau}$ where $\mathcal{R}_2(\alpha)$ given in (29). Then, the positive equilibria of (38) are determined by $\hat{\mathcal{R}}_2(\alpha,\tau)e^{-ax_x} - 1 = 0$ and $e^{ax_2} - W(\alpha) = 0$. Observe that like $\mathcal{R}_1(\alpha)$, $\hat{\mathcal{R}}_1(\alpha,\tau)$ remain decreasing on $[s_2/s_2, b_0/b_1)$, and $\hat{\mathcal{R}}_2(\alpha,\tau)$ and $\mathcal{R}_2(\alpha)$ share the same monotonicity/nonmonotonicity and $[0, s_2/s_3)$. Also note that the equations for $\alpha'(t)$ in each of the three intervals for α remain the same as for the case of $\tau = 0$.

Based on the above observations, we can similarly discuss the structure of equilibria. Firstly, there is the no-fear positive equilibrium $E_s(\bar{x}_{20}, 0)$ if $\hat{\mathcal{R}}_2(0,\tau) > 1$. However, when it comes to interior equilibria, a new phenomenon occurs: There may be *two* interior equilibria. To see this, we first note that $\hat{\mathcal{R}}_2(\alpha,\tau)$ has the same monotonicity/nonmonotonicity in α as $\mathcal{R}_2(\alpha)$ does, which is determined by whether $W(0) > \mathcal{R}_2(0)$ or $W(0) < \mathcal{R}_2(0)$. If $W(0) > \mathcal{R}_2(0)$, both $\mathcal{R}_2(\alpha)$ and $\hat{\mathcal{R}}_2(\alpha,\tau)$ are decreasing on $[0, s_2/s_3)$, and thus, $\hat{\mathcal{R}}_2(\alpha,\tau) \le \hat{\mathcal{R}}_2(0,\tau) \le \mathcal{R}_2(0) < W(0) < W(\alpha)$, implying that there cannot be an interior equilibrium. Thus, $W(0) < \mathcal{R}_2(0)$ is still a necessary condition for existence of an interior equilibrium of the model. Assuming $W(0) < \mathcal{R}_2(0)$, then both $\mathcal{R}_2(\alpha)$ and $\hat{\mathcal{R}}_2(\alpha,\tau)$ are one hump functions on $[0, s_2/s_3)$ (both attaining their maxima at α^*) and in the mean time $\hat{\mathcal{R}}_2(0,\tau) < W(0)$ for properly chosen $\tau > 0$, giving rise to two interior equilibria. See Fig. 6 for an illustration, showing the impact of the delay $\tau > 0$ on existence/nonexistence of interior equilibria: Under $W(0) < \mathcal{R}_2(0)$, there can be one, two, or no interior equilibrium, as τ increases.

As in the previous subsection, we now analytically explore the existence of interior equilibrium $E(\bar{x}_2, \bar{\alpha})$. Again letting $\psi = e^{-ax_2}$ and solving $W(\alpha) = e^{ax_2} = 1/\psi$, we still have (30). By plugging the formula for $\bar{\alpha}$ in (30) into $\hat{\mathcal{R}}_2(\bar{\alpha},\tau) = 1/\psi$ and solving for ψ, we find that ψ is determined by

$$F(\psi) := \rho_1\,\psi^2 + \rho_2\,\psi + \rho_3 = 0. \tag{39}$$

Here in (39) we have

$$\begin{aligned}
\rho_1 &= -b_1^2\left(b_1^2\,d_2 + y\,(b_1\,s_2 - b_0\,s_3)^2\right),\\
\rho_2 &= y\,s_3^2\left(e^{-p\,\tau}\,y\,(b_0\,s_3 - b_1\,s_2)^2 + 2\,b_1^2\,d_2\right), \quad \rho_3 = -d_2\,y^2\,s_3^4.
\end{aligned} \tag{40}$$

Similar arguments to that in Sect. 4.2.1 still hold here, and thus, we need to look for real roots of (39) in the interval $(0, \psi_0)$ where ψ_0 is given in (32). Let

$$\Delta = \rho_2^2 - 4\,\rho_1\,\rho_3. \tag{41}$$

المنارة للاستشارات

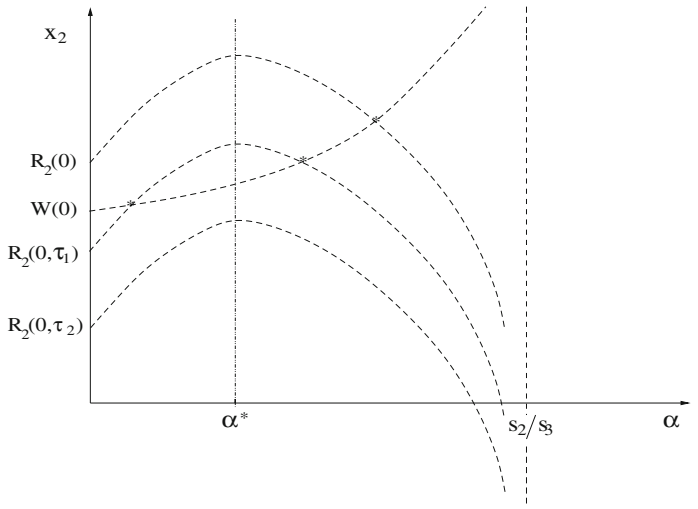

Fig. 6 Impact of $\tau > 0$ on the number of interior equilibria, assuming $W(0) < \mathcal{R}_2(0)$: There can be one, two, and no interior equilibrium, when $\tau = 0$, τ_1, and τ_2, respectively, where $0 < \tau_1 < \tau_2$

From (40), it is obvious that $\rho_1 < 0$, $\rho_2 > 0$, $\rho_3 < 0$; thus, $F(0) = \rho_3 < 0$ and $F'(0) = \rho_2 > 0$. Therefore, (39) has no positive root if $\Delta < 0$, (39) has one positive equilibrium if $\Delta = 0$, and (39) has two distinct positive roots if $\Delta > 0$. For the last case, denote the two positive roots of (39) by ψ_1, ψ_2, respectively, and assume $\psi_1 < \psi_2$ without loss of generality. Thus, system (24) admits a unique positive equilibrium ψ_1 if $\Delta = 0$, $\psi_1 = \psi_2 < \psi_0$, or $\Delta > 0$ but $\psi_1 < \psi_0 < \psi_2$, and it has two distinct equilibria if $\Delta > 0$ and $\psi_2 < \psi_0$.

The above results can be restated in terms of a particularly chosen parameters for its range(s). For example, if we choose τ, then Fig. 6 clearly demonstrates how the values of $\tau > 0$ are related to the above-mentioned conditions. If we choose d_2, then the condition $\Delta = 0$ is equivalent to

$$d_2 = \frac{y\left(e^{-p\tau}\right)^2 (b_0 s_3 - b_1 s_2)^2}{4 b_1^2 \left(1 - e^{-p\tau}\right)} := d_2^0. \tag{42}$$

Moreover, if we denote d_2^1 by

$$d_2^1 := \frac{\psi_0 y (b_0 s_3 - b_1 s_2)^2 \left(e^{-p\tau} s_3^2 y - \psi_0 b_1^2\right)}{\left(b_1^2 \psi_0 - s_3^2 y\right)^2} \tag{43}$$

for convenience, then the above analytical results about the existence of interior equilibrium/equilibria can be restated in the following two theorems.

المنارة للاستشارات

Theorem 4.5 *Assume that (33) (necessary condition) holds. Then, (24) has a unique interior equilibrium* $E_{p1} = (\bar{x}_{21}, \bar{\alpha}_1)$ *if either*

$$\begin{cases} e^{-p\tau} < \dfrac{2\,\psi_0\,b_1^2}{y\,s_3^2 + \psi_0\,b_1^2}, \\ d_2 = d_2^0; \end{cases} \tag{44}$$

or

$$\begin{cases} e^{-p\tau} > \dfrac{\psi_0\,b_1^2}{s_3^2\,y}, \\ d_2 < d_2^1 \end{cases} \tag{45}$$

where

$$\bar{x}_{21} = \frac{-1}{a}\ln\left(\frac{-\rho_2 + \sqrt{\Delta}}{2\,\rho_1}\right), \quad \bar{\alpha}_1 = \frac{b_0\,b_1\left(\left(-\rho_2 + \sqrt{\Delta}\right)/(2\,\rho_1)\right) - s_2\,s_3\,y}{b_1^2\left(\left(-\rho_2 + \sqrt{\Delta}\right)/(2\,\rho_1)\right) - s_3^2\,y}. \tag{46}$$

Theorem 4.6 *Two distinct positive equilibria* $E_{p1} = (\bar{x}_{21}, \bar{\alpha}_1)$, $E_{p2} = (\bar{x}_{22}, \bar{\alpha}_2)$ *of (24) exist if*

$$\begin{cases} e^{-p\tau} \le \dfrac{\psi_0\,b_1^2}{s_3^2\,y}, \\ d_2 < d_2^0; \end{cases} \tag{47}$$

or

$$\begin{cases} \dfrac{\psi_0\,b_1^2}{s_3^2\,y} < e^{-p\tau} < \dfrac{2\,\psi_0\,b_1^2}{b_1^2\,\psi_0 + s_3^2\,y}, \\ d_2^1 < d_2 < d_2^0, \end{cases} \tag{48}$$

where $\bar{x}_{21}$, $\bar{\alpha}_1$ *are the same as (46), and*

$$\bar{x}_{22} = \frac{-1}{a}\ln\left(\frac{-\rho_2 - \sqrt{\Delta}}{2\,\rho_1}\right), \quad \bar{\alpha}_2 = \frac{b_0\,b_1\left(\left(-\rho_2 - \sqrt{\Delta}\right)/(2\,\rho_1)\right) - s_2\,s_3\,y}{b_1^2\left(\left(-\rho_2 - \sqrt{\Delta}\right)/(2\,\rho_1)\right) - s_3^2\,y}. \tag{49}$$

4.2.3 Stability of Equilibria for System (24) with $\tau > 0$

We begin with analyzing local stability of the semi-trivial equilibrium E_s which exists under the assumption $\hat{\mathcal{R}}_2(0, \tau) > 1$. The linearization of (24) at E_s is

$$\begin{aligned} \frac{\mathrm{d}x_2}{\mathrm{d}t} &= f_{11}\,x_2 + f_{12}\,\alpha + f_{13}\,x_2(t-\tau) + f_{14}\,\alpha(t-\tau), \\ \frac{\mathrm{d}\alpha}{\mathrm{d}t} &= f_{22}\,\alpha, \end{aligned} \tag{50}$$

المنارة للاستشارات

where

$$
\begin{aligned}
f_{11} &= -d_2 - s_2^2\, y,\\
f_{12} &= 2\, s_2\, s_3\, \bar{x}_{20}\, y,\\
f_{13} &= \left(d_2 + s_2^2\, y\right)(1 - a\bar{x}_{20}),\\
f_{14} &= -2\, b_1\, \bar{x}_{20} \left(\frac{d_2 + s_2^2\, y}{b_0}\right),\\
f_{22} &= k\, \bar{x}_{20} \left(-2\, b_0\, b_1\, e^{-a\, \bar{x}_{20}} + 2\, s_2\, s_3\, y\right).
\end{aligned} \tag{51}
$$

Plugging $(x_2,\, \alpha) = e^{(\lambda\, t)}(v_1,\, v_2)$ into (50), we obtain the characteristic equation at E_s

$$G(\lambda,\, \tau) := \left[\lambda - \left(f_{11} + f_{13}\, e^{-\lambda\, \tau}\right)\right](\lambda - f_{22}) = 0. \tag{52}$$

The following theorem gives conditions for the asymptotical stability of E_s.

Theorem 4.7 *Assume $\hat{\mathcal{R}}_2(0, \tau) > 1$ so that E_s exists. Then, E_s is locally asymptotically stable if*

$$\hat{\mathcal{R}}_2(0, \tau) < \frac{b_0\, b_1}{s_2\, s_3\, y} \quad \textit{and} \quad \hat{\mathcal{R}}_2(0, \tau) \le e^2. \tag{53}$$

Proof Noting that $\bar{x}_{20} = \frac{1}{a} \ln \hat{\mathcal{R}}_2(0, \tau)$, one root of the characteristic equation (52) is real and given by

$$\lambda = f_{22} = -2\, k\, \bar{x}_{20} \left(\frac{b_0\, b_1}{\hat{\mathcal{R}}_2(0, \tau)} - s_2\, s_3\, y\right)$$

which is negative if and only if

$$\hat{\mathcal{R}}_2(0, \tau) < \frac{b_0\, b_1}{s_2\, s_3\, y}. \tag{54}$$

All other eigenvalues of (52) are determined by

$$D(\lambda, \tau) := P(\lambda, \tau) + Q(\lambda, \tau)\, e^{-\lambda\, \tau} = 0, \tag{55}$$

where

$$
\begin{aligned}
P(\lambda, \tau) &= \lambda - f_{11} = \lambda + \left(d_2 + s_2^2\, y\right),\\
Q(\lambda, \tau) &= -f_{13} = -\left(d_2 + s_2^2\, y\right)(1 - a\, \bar{x}_{20}).
\end{aligned} \tag{56}
$$

Because $D(0, \tau) = \left(d_2 + s_2^2\, y\right) a\bar{x}_{20} > 0$, $\lambda = 0$ is not a characteristic root of (55) for any $\tau > 0$. Observe that E_s is asymptotically stable when $\tau = 0$

المنارة للاستشارات

by Theorem 4.3. Therefore, stability of E_s can change only through the occurrence of pure imaginary roots of (55). Assume $\lambda = i\,\omega$ with $\omega > 0$. Because $|P(i\,\omega,\tau)| = |-Q(i\,\omega,\tau)\,\exp(-i\,\omega\,\tau)| = |Q(i\,\omega,\tau)|$ (by (55)), $\omega > 0$ must satisfy

$$\begin{aligned} 0 = F(\omega,\tau) &= |P(i\,\omega,\tau)|^2 - |Q(i\,\omega,\tau)|^2 \\ &= \omega^2 + \left(d_2 + s_2^2\,y\right)^2 - \left(d_2 + s_2^2\,y\right)^2 (1 - a\,\bar{x}_{20})^2 \\ &= \omega^2 + \left(d_2 + s_2^2\,y\right)^2 \left[1 - (1 - a\bar{x}_{20})^2\right]. \end{aligned} \tag{57}$$

Obviously, (57) has no positive solution if $a\bar{x}_{20} \le 2$, implying that there is no pure imaginary root for (55). Simple calculation shows that

$$a\,\bar{x}_{20} \le 2 \Longleftrightarrow \hat{\mathcal{R}}_2(0,\tau) \le e^2. \tag{58}$$

Indeed, if (58) holds, then (55) also has no root with *positive real part*. To see this, we assume $\lambda = r + i\,\omega$ is a root of (55) with $r > 0$ and $\omega > 0$. By substituting $\lambda = r + i\,\omega$ into (55), we obtain

$$r + \left(d_2 + s_2^2\,y\right) + i\,\omega = \left(d_2 + s_2^2\,y\right)(1 - a\,\bar{x}_{20})e^{-r\,\tau}e^{-i\,\omega\,\tau},$$

which gives

$$\left|r + \left(d_2 + s_2^2\,y\right) + i\,\omega\right| = \left|\left(d_2 + s_2^2\,y\right)(1 - a\,\bar{x}_{20})e^{-r\,\tau}e^{-i\,\omega\,\tau}\right|. \tag{59}$$

Because $r > 0$ by assumption, (59) implies

$$\begin{aligned} &\left(d_2 + s_2^2\,y\right)^2 < \left(r + d_2 + s_2^2\,y\right)^2 < \left(r + d_2 + s_2^2\,y\right)^2 + \omega^2 \\ &= \left(d_2 + s_2^2\,y\right)^2 (1 - a\,\bar{x}_{20})^2\,e^{-2r\,\tau} < \left(d_2 + s_2^2\,y\right)^2 (1 - a\,\bar{x}_{20})^2, \end{aligned} \tag{60}$$

implying that $2 < a\,\bar{x}_{20}$ which contradicts to (58). Therefore, every eigenvalue $\lambda = r + i\,\omega$ of (55) must have $r < 0$ if (58) holds. As a consequence, local stability of E_s remains valid for $\tau > 0$ if (54) and (58) hold. □

Remark 4.8 If one wants to explore the impact of the delay, the conditions in Theorem 4.7 can be actually explicitly expressed in terms of τ as follows:

$$\hat{\mathcal{R}}_2(0,\tau) > 1 \Leftrightarrow \tau < \frac{1}{p}\ln\left(\frac{b_0^2}{d_2 + s_2^2\,y}\right), \tag{61}$$

$$\hat{\mathcal{R}}_2(0,\tau) < \min\left\{\frac{b_0\,b_1}{s_2\,s_3\,y}, e^2\right\} \Leftrightarrow \frac{1}{p}\ln\left(\frac{b_0^2}{\min\left\{(b_0\,b_1)/(s_2\,s_3\,y), e^2\right\}\left(d_2 + s_2^2\,y\right)}\right) < \tau. \tag{62}$$

المنارة للاستشارات

Noting that $\hat{\mathcal{R}}_2(0,\tau)$ is decreasing in τ, we immediately have the following corollary.

Corollary 4.9 *Assume that*

$$\frac{b_0^2}{d_2+s_2^2 y} < \min\left\{\frac{b_0 b_1}{s_2 s_3 y},\ e^2\right\}.$$

Then, E_s is asymptotically stable as long as it exists (i.e., provided that $\hat{\mathcal{R}}_2(0,\tau) > 1$.)

From the proof of Theorem 4.7, we can see that violation of condition (54) leads to the sign change of a real eigenvalue from negative to positive, and loss of stability of E_s results in the occurrence of a positive equilibrium (see the condition (45) in Theorem 4.5), which will be discussed later. The violation of the other condition (58), on the other hand, makes it possible for a pair of complex eigenvalues to cross the imaginary axis from the left half plane to the right in the complex plane, and this is expected to cause Hopf bifurcation. We explore a bit more along this line as follows. The focus is on the impact of the delay $\tau > 0$, and accordingly, we assume that the conditions in Theorem 4.3 hold so that E_s is asymptotically stable when $\tau = 0$, and we follow the framework of Beretta and Kuang (2002) to proceed.

Assume the opposite of (58), that is

$$a\,\bar{x}_{20} > 2 \quad \left(\text{equivalently } \hat{\mathcal{R}}_2(0,\tau) > e^2\right). \tag{63}$$

Under (63), Eq. (57) admits a unique positive root given by

$$\omega(\tau) = \left(d_2 + s_2^2\, y\right)\sqrt{(1-a\,\bar{x}_{20})^2 - 1}. \tag{64}$$

Following Beretta and Kuang (2002), let I denote the interval in which $\omega(\tau)$ in (64) is defined. Solving (63) for τ then gives

$$I = \left[0,\ \frac{1}{p}\ln\frac{b_0^2}{\left(d_2+s_2^2 y\right)e^2}\right).$$

Let $\theta(\tau):\ I \to \mathbb{R}_+$ be the solution of

$$\sin\theta(\tau) = -\frac{\omega(\tau)}{\left(d_2+s_2^2\, y\right)(1-a\,\bar{x}_{20})},\quad \cos\theta(\tau) = \frac{1}{1-a\,\bar{x}_{20}}. \tag{65}$$

Then, by Beretta and Kuang (2002), stability switch of E_s may occur when τ is a zero of

$$S_n(\tau) := \tau - \frac{\theta(\tau)+n\,2\pi}{\omega(\tau)},\quad \tau \in I,\quad n \in \mathbb{N}. \tag{66}$$

المنارة للاستشارات

To finally confirm the stability switch, we need to verify the transversality condition at zeros of $S_n(\tau)$, $\tau \in I$. To this end, we use the implicit differentiation in (55) to obtain

$$\frac{\mathrm{d}\lambda}{\mathrm{d}\tau} = \frac{(f_{13}^{'} - f_{13}\,\lambda)e^{-\lambda\tau}}{1 + f_{13}\,\tau\,e^{-\lambda\,\tau}}, \tag{67}$$

where f_{13} is shown in (51). We point out that it is more convenient to consider

$$\left(\frac{\mathrm{d}\lambda}{\mathrm{d}\tau}\right)^{-1} = \frac{e^{\lambda\tau} + f_{13}\,\tau}{f_{13}^{'} - f_{13}\lambda} = \frac{f_{13}/(\lambda - f_{11}) + f_{13}\tau}{f_{13}^{'} - f_{13}\lambda}. \tag{68}$$

At a zero τ^* of $S_n(\tau)$, we have $\lambda(\tau^*) = i\,w(\tau^*)$. This observation together with (55) and (57) helps us to simplify (68) to

$$\begin{aligned}\left(\frac{\mathrm{d}\lambda}{\mathrm{d}\tau}\right)^{-1}\Big|_{\lambda=i\,\omega(\tau_i)} &= \frac{-f_{11} + f_{13}^2\,\tau - \omega\,i}{\omega\,\omega^{'} - f_{13}^2\,\omega\,i} \\ &= \frac{1}{\omega^2\,\omega^{'2} + f_{13}^4\,\omega^2}\left(\left(-f_{11} + f_{13}^2\,\tau\right)\omega\,\omega^{'}\right. \\ &\quad \left. + \omega^2\,f_{13}^2 + \left(f_{13}^2\,\omega - \omega^2\,\omega^{'}\right)i\right).\end{aligned} \tag{69}$$

By (69), we obtain

$$\frac{\mathrm{d}\,\mathrm{Re}(\lambda)}{\mathrm{d}\tau}\Big|_{\lambda=i\,\omega(\tau_i)} = \frac{\left(-f_{11} + f_{13}^2\,\tau\right)\omega\,\omega' + \omega^2\,f_{13}^2}{\omega^2\,\omega^{'2} + f_{13}^4\,\omega^2}. \tag{70}$$

The formula in (70) can be used to determine the transversality for Hopf bifurcation. Unfortunately, we cannot confirm the sign of this formula for general model parameters. However, once the values of parameters are given, it is straightforward and easy to numerically calculate the zeros of $S_n(\tau)$ and evaluate (70) at these zeros and therefore determine whether Hopf bifurcation will occur. For example, for parameters chosen in Fig. 7, by numerically solving $S_n(\tau) = 0$, we find that there are two zeros for $S_0(\tau)$, which are $\tau_1 = 0.5$ and $\tau_2 = 4.782$, as shown in Fig. 7, but none for $S_n(\tau)$, $n = 1, \ldots$. Moreover, numerical evaluations of (70) at τ_1 and τ_2 indicate that $\mathrm{d}\,\mathrm{Re}(\lambda)/\mathrm{d}\tau > 0$ at τ_1 and $\mathrm{d}\,\mathrm{Re}(\lambda)/\mathrm{d}\tau < 0$ at τ_2. This implies that the model (24) undergoes Hopf bifurcation at these two critical values: When τ increases to pass τ_1, E_s loses its stability leading to sustained oscillation of the population; while when τ further increases to pass τ_2, the periodic solutions disappear and E_s regains its stability. These are confirmed by numerical simulations of the model (24), as shown in Fig. 8.

The above analyses have shown that the semi-trivial equilibrium E_s may lose its stability to a stable periodic solution with an intermediate value of τ and regain its stability when τ is large, through Hopf bifurcation. Note that the Hopf bifurcations occurred are local, i.e., periodic orbits bifurcate from E_s near the bifurcation parameters τ_1 and τ_2. However, under suitable conditions, global Hopf bifurcation may occur

المنارة للاستشارات

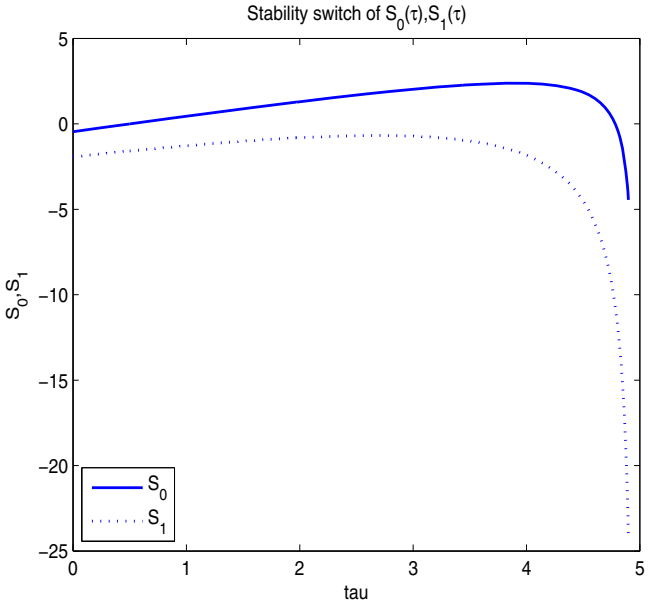

Fig. 7 Stability switch of E_s. Parameters are: $b_0 = 8.1311$, $b_1 = 9.1252$, $a = 0.9858$, $p = 0.3290$, $s_2 = 1.3924$, $s_3 = 2.4989$, $y = 0.5376$, $d_2 = 0.7139$, $k = 1$

and multiple periodic solutions with different frequencies may coexist within a certain range of τ. Detailed analysis and numerical simulations of global Hopf bifurcation and Hopf branches in terms of the bifurcation parameters can be found in Shu et al. (2013) and are thus omitted here.

In addition to this, as we mentioned before, E_s may also lose its stability to a positive equilibrium through equilibrium bifurcation. This is due to the violation of the first condition in (53) and is reflected by a real eigenvalue crossing the pure imaginary axis from the left to the right in the complex plane. Such a positive equilibrium is interesting since it represents a persistent anti-predator defense. Thus, the stability/instability of such a positive equilibrium is of great importance.

Note that Theorems 4.5 and 4.6 have confirmed that one positive equilibrium or two positive equilibria may exist under different conditions. However, if $\tau = 0$, E_{p2} in Theorem 4.6 cannot exist because the conditions for its existence are contradictory in this case. Hence, we first consider the case when a unique positive equilibrium E_{p1} exists (i.e., when conditions in Theorem 4.5 hold) for $\tau \geq 0$ and then proceed to the case where Theorem 4.6 holds by restricting $\tau > 0$. The procedure is exactly the same as the one for the stability/instability of E_s above, mainly using the framework in Beretta and Kuang (2002), as such we will try to be brief as follows, omitting many details.

By linearizing (24) at E_{p1}, we obtain characteristic equation at E_{p1}:

$$G(\lambda, \tau) := \lambda^2 - (g_{11} + g_{22})\,\lambda + (g_{11}\,g_{22} - g_{21}\,g_{12}) + (-g_{13}\,\lambda + g_{13}\,g_{22} - g_{21}\,g_{14})\,e^{-\lambda\,\tau} = 0, \tag{71}$$

المنارة للاستشارات

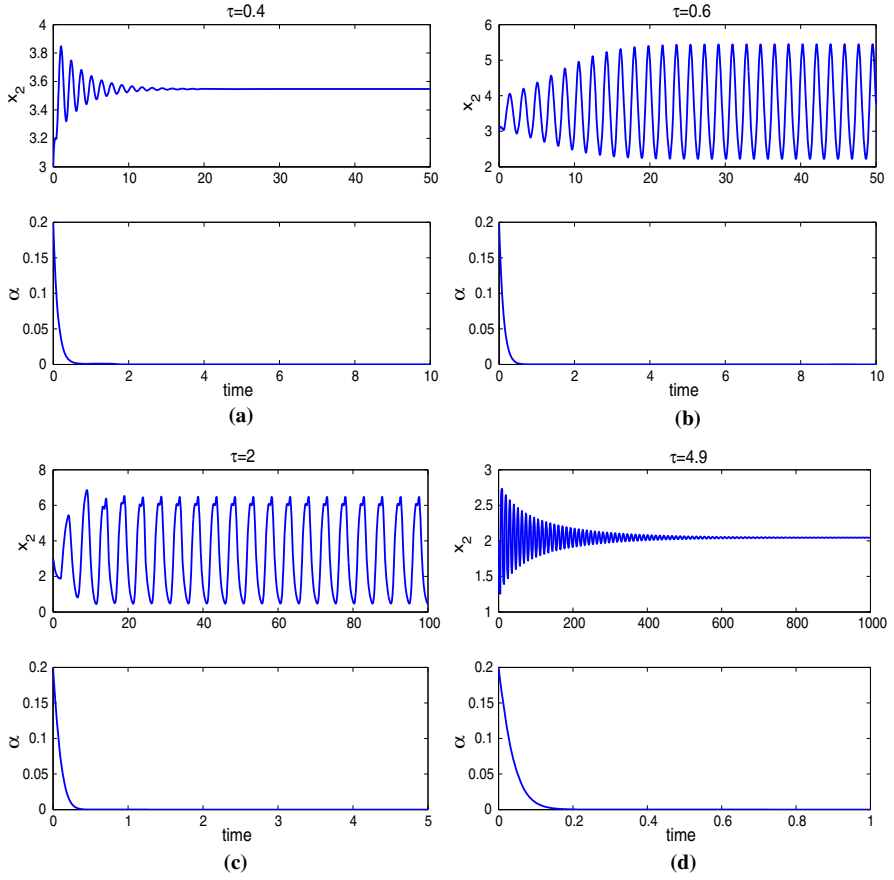

Fig. 8 Stability switch of E_s with varying τ. Parameters are: $b_0 = 8.1311$, $b_1 = 9.1252$, $a = 0.9858$, $p = 0.3290$, $s_2 = 1.3924$, $s_3 = 2.4989$, $y = 0.5376$, $d_2 = 0.7139$, $k = 1$. **a** Small delay, **b** intermediate delay, **c** intermediate delay, **d** large delay

where

$$
\begin{aligned}
g_{11} &= -d_2 - (s_2 - s_3\,\bar{\alpha}_1)^2\,y,\\
g_{12} &= 2\,s_3\,(s_2 - s_3\,\bar{\alpha}_1)\bar{x}_{21}\,y,\\
g_{13} &= (b_0 - b_1\,\bar{\alpha}_1)^2\,e^{-a\,\bar{x}_{21}}\,e^{-p\,\tau}(1 - a\,\bar{x}_{21}),\\
g_{14} &= -2\,(b_0 - b_1\,\bar{\alpha}_1)\,e^{-a\,\bar{x}_{21}}\,\bar{x}_{21}\,e^{-p\,\tau}\,b_1,\\
g_{21} &= 2\,k\,\bar{\alpha}_1(1 - \bar{\alpha}_1)\,a\,s_3\,(s_2 - s_3\,\bar{\alpha}_1)\,y\,\bar{x}_{21},\\
g_{22} &= 2\,k\,\bar{x}_{21}\,\bar{\alpha}_1\,(1 - \bar{\alpha}_1)\,\left(b_1^2\,e^{-a\,\bar{x}_{21}}\,\bar{x}_{21} - s_3^2\,y\right).
\end{aligned}
\tag{72}
$$

When $\tau = 0$, the results for the stability of E_{p1} can be found in Theorem 4.4. Again, we hope to see whether delay τ would induce stability switch of E_{p1}. Assuming that the conditions in Theorem 4.4 hold so that E_{p1} is stable when $\tau = 0$. We seek pure

imaginary root $i\,\omega$ of (71) to examine possible stability switch of E_{p1} when $\tau > 0$. Similar to the proof of Theorem 4.7, we substitute $i\,\omega$ with $\omega > 0$ into (71) and obtain

$$F(\omega,\,\tau) = \omega^4 - \omega^2\left(g_{13}^2 + 2\,(g_{11}\,g_{22} - g_{21}\,g_{12}) - (g_{11} + g_{22})^2\right) + \left((g_{11}\,g_{22} - g_{21}\,g_{12})^2 - (g_{13}\,g_{22} - g_{21}\,g_{14})^2\right) = 0, \tag{73}$$

where $g_{11},\ g_{12},\ g_{13},\ g_{14},\ g_{21},\ g_{22}$ are shown in (72). Let

$$\Delta = \left[g_{13}^2 + 2\,(g_{11}\,g_{22} - g_{21}\,g_{12}) - (g_{11} + g_{22})^2\right]^2 - 4\left[(g_{11}\,g_{22} - g_{21}\,g_{12})^2 - (g_{13}\,g_{22} - g_{21}\,g_{14})^2\right]. \tag{74}$$

By (74), we know that (73) admits two positive equilibria $\omega_1^2,\ \omega_2^2$ with $\omega_1^2(\tau) < \omega_2^2(\tau)$ if $\Delta > 0$, where

$$\omega_1^2(\tau) = \frac{1}{2}\left[\left(g_{13}^2 + 2\,(g_{11}\,g_{22} - g_{21}\,g_{12}) - (g_{11} + g_{22})^2\right) - \sqrt{\Delta}\right],$$
$$\omega_2^2(\tau) = \frac{1}{2}\left[\left(g_{13}^2 + 2\,(g_{11}\,g_{22} - g_{21}\,g_{12}) - (g_{11} + g_{22})^2\right) + \sqrt{\Delta}\right]. \tag{75}$$

We first consider possible stability switch of E_{p1} where only ω_2^2 exists. Similar to (65) and (66), define $\theta(\tau) \in [0,\ 2\,\pi)$ such that

$$\sin(\theta(\tau)) = \frac{\left((g_{11}\,g_{22} - g_{21}\,g_{12}) - \omega_2^2\right)\,\omega_2\,g_{13} - \omega_2\,(g_{11} + g_{22})\,(g_{13}\,g_{22} - g_{21}\,g_{14})}{\omega_2^2\,g_{13}^2 + (g_{13}\,g_{22} - g_{21}\,g_{14})^2},$$
$$\cos(\theta(\tau)) = -\frac{\left((g_{11}\,g_{22} - g_{21}\,g_{12}) - \omega_2^2\right)\,(g_{13}\,g_{22} - g_{21}\,g_{14}) + \omega_2^2\,(g_{11} + g_{22})\,g_{13}}{\omega_2^2\,g_{13}^2 + (g_{13}\,g_{22} - g_{21}\,g_{14})^2}. \tag{76}$$

Then stability switch of E_{p1} occurs when τ passes zeros of

$$S_n^0(\tau) := \tau - \frac{\theta(\tau) + n\,2\,\pi}{\omega_2(\tau)},\quad n \in \mathbb{N}, \tag{77}$$

where θ is obtained by solving (76). Based on Beretta and Kuang (2002) and again employing numerical tools, zeros of (77) can be obtained. For example, for the set of parameter values in Fig. 9, by numerically solving $S_0^0(\tau) = 0$, we obtain two zeros $\tau_1 = 0.123$ and $\tau_2 = 0.154$, as shown in Fig. 9. Because E_{p1} is locally stable when $\tau = 0$, E_{p1} switches from stable to unstable when τ increase to pass $\tau_1 = 0.123$. Again, numerical simulation of the model, as shown in Fig. 10, confirms that when maturation delay τ is relatively small, the local stability of E_{p1} will not change. However, if τ is larger ($\tau > \tau_1$), delay will destroy the stability of E_{p1} causing

المنارة للاستشارات

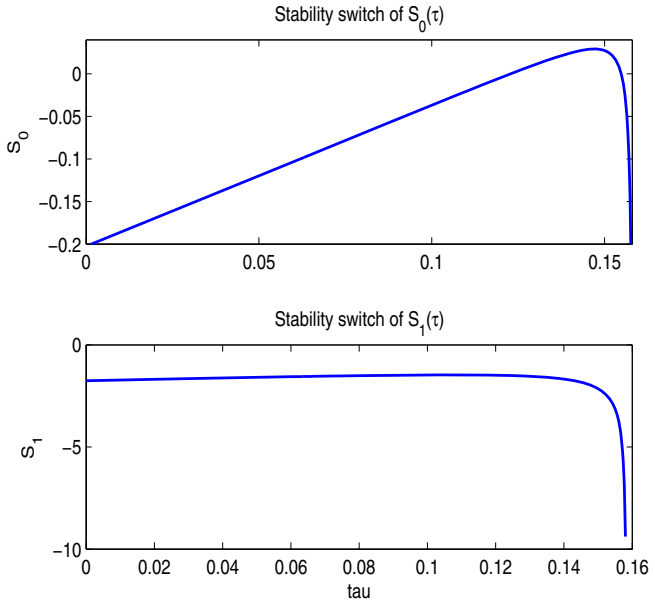

Fig. 9 Stability switch of E_{p1} where only E_{p1} exists as a positive equilibrium. Parameters are: $b_0 = 3.07552$, $b_1 = 4.33876$, $a = 0.38976$, $p = 0.750396$, $s_2 = 0.562070$, $s_3 = 1.21206$, $y = 4.89360$, $d_2 = 0.552225$, $k = 31.0047$

periodic oscillations for *both* x_2 and α (in contrast to the situation when E_s loses stability due to Hopf bifurcation in which only $x_2(t)$ oscillates), as demonstrated in Fig. 10b, c. When τ further increases to pass the second critical value τ_2 shown in Fig. 9, E_{p1} regains its stability and both $(x_2(t), \alpha(t))$ tend to the equilibrium E_{p1} again, as indicated in Fig. 10d. Here in (77), only $S_0^0(\tau) = 0$ has real roots. Hence there are no other critical values of τ other than τ_1 and τ_2 that could induce stability switch of E_{p1}. We point out that parameters chosen in Fig. 9 only admit positive $\omega_2^2(\tau)$, but $\omega_1^2(\tau)$ is negative and hence only allows a unique positive equilibrium of (73). Although we cannot prove analytically, our extensive numerical simulations show that $\omega_1^2(\tau)$ is always negative.

As for the case when there are two positive equilibria E_{p1} and E_{p2} under the conditions in Theorem 4.6, by numerical simulations, we find that under such conditions, E_{p2} is always unstable. In this case, going through the same procedure of constructing $S_n^0(\tau)$ and numerically solving $S_n^0(\tau) = 0$ reveal that the delay-induced instability of E_{p1} is different from the previous case where E_{p2} does not exist. As shown in Fig. 11, $S_n^0(\tau)$ has only a unique positive root, which is different from Fig. 9 where two distinct positive roots of $S_n^0(\tau)$ exist. Accordingly, E_{p1} will remain asymptotically stable when $\tau > 0$ and is small, and will lose its stability to a periodic solution when τ increases to pass the unique critical value $\tau_c > 0$ through Hopf bifurcation; however, E_{p1} cannot regain its stability through Hopf bifurcation. These numerical observations are illustrated in Fig. 12, where the parameters give a unique $\tau_c \approx 2$ from $S_0^0(\tau) = 0$.

المنارة للاستشارات

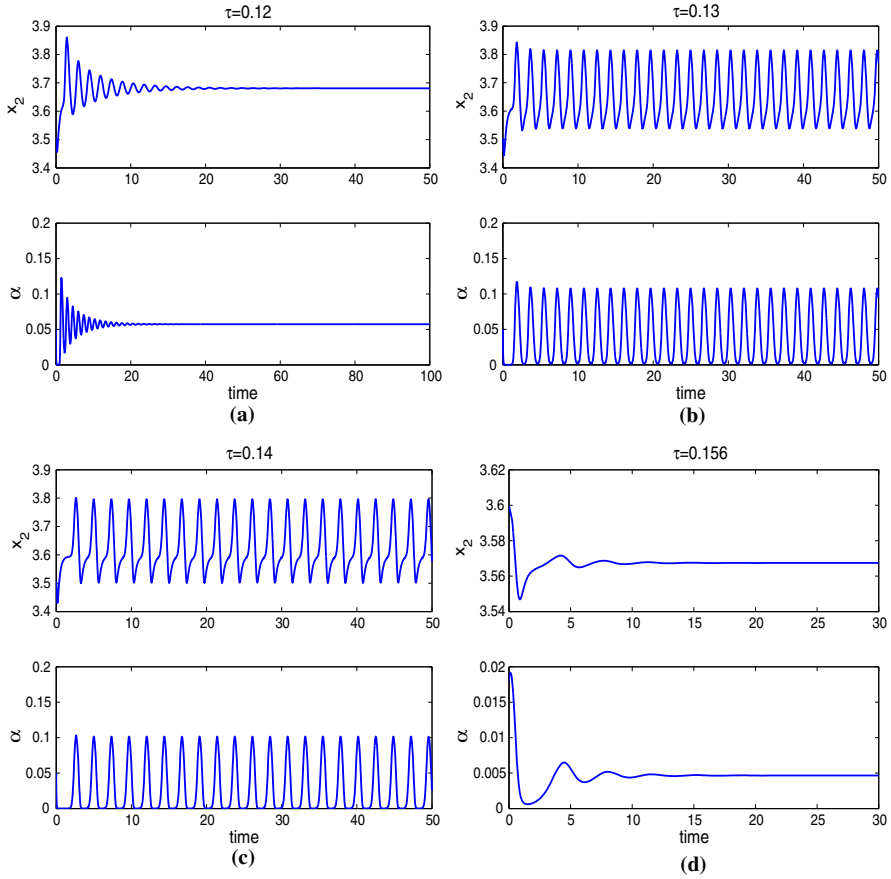

Fig. 10 Stability switch of E_{p1} with varying τ. Parameters are: $b_0 = 3.07552, b_1 = 4.33876, a = 0.38976, p = 0.750396, s_2 = 0.562070, s_3 = 1.21206, y = 4.89360, d_2 = 0.552225, k = 31.0047$. **a** Small delay, **b** intermediate delay, **c** intermediate delay, **d** large delay

4.3 Full Model

In this section, we consider the original 3-d model (6). Since the full model involves three equations with delays and is much more complicated, we will mainly explore it numerically. Before that and in order to simplify the notations, let $p = d_0 + s_0\, y$, $q = d_1 + s_1\, y$. Similar to the analysis of the reduced 2-d model (24) and still making use of the same $\hat{\mathcal{R}}_2(\alpha, \tau)$, we may determine the existence of a semi-trivial equilibrium of (6), as stated in the following lemma.

Lemma 4.1 *A semi-trivial equilibrium* $E_{s0} = (\bar{x}_{10}, \bar{x}_{20}, 0)$ *exists if*

$$\hat{\mathcal{R}}_2(0, \tau) > 1, \quad \tau > 0, \tag{78}$$

المنارة للاستشارات

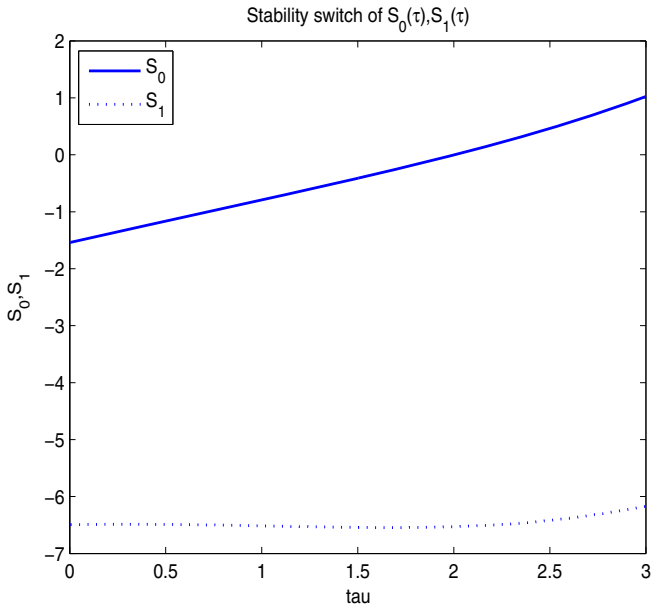

Fig. 11 Stability switch of E_{p1} where both E_{p1} and E_{p2} may exist. Parameters are: $b_0 = 4.6332, b_1 = 5.4762, a = 0.1694, p = 0.3781, d_2 = 0.5693, s_2 = 0.5797, s_3 = 3.7623, y = 4.7052, k = 0.7519$

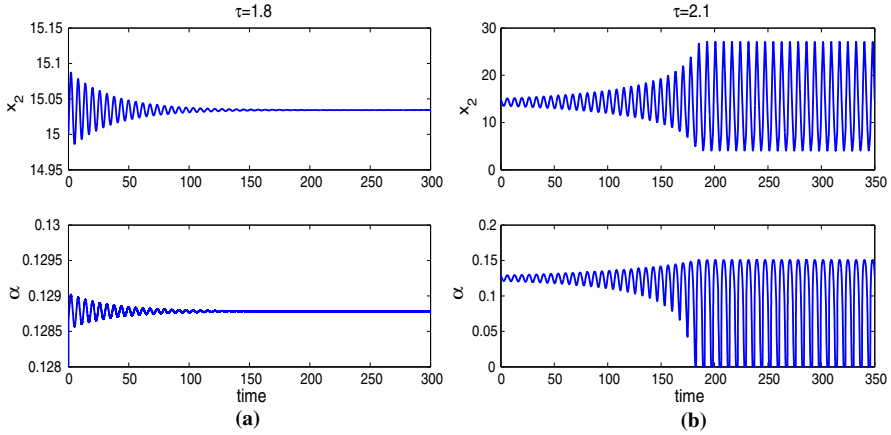

Fig. 12 Stability switch of E_{p1} with varying τ. Parameters are: $b_0 = 4.6332, b_1 = 5.4762, a = 0.1694, p = 0.3781, d_2 = 0.5693, s_2 = 0.5797, s_3 = 3.7623, y = 4.7052, k = 0.7519$. **a** Small delay and **b** large delay

where

$$\bar{x}_{10} = \frac{\left(d_2 + s_2^2\, y\right)\left(e^{p\,\tau} - 1\right)}{a\; p} \ln \hat{\mathcal{R}}_2(0, \tau),$$
$$\bar{x}_{20} = \frac{1}{a} \ln \hat{\mathcal{R}}_2(0, \tau). \tag{79}$$

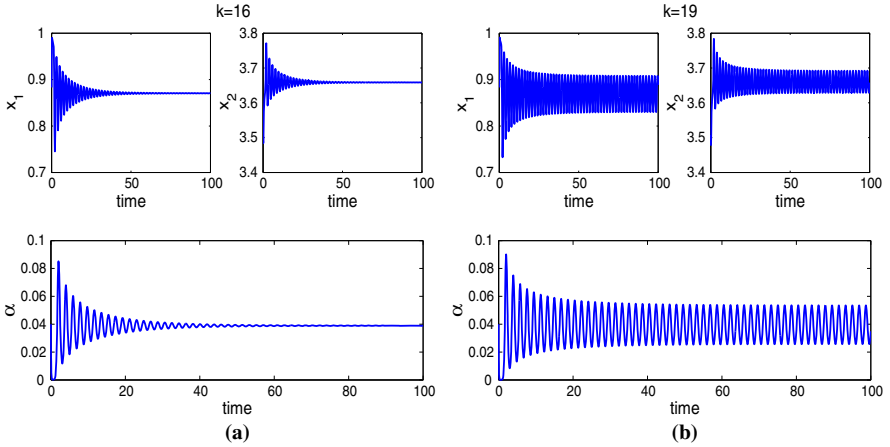

Fig. 13 Steady state or oscillation of system (6) with varying k. Parameters are: $b_0 = 3.07552, b_1 = 4.33876, a = 0.38976, p = 0.750396, q = 0.2, s_2 = 0.562070, s_3 = 1.21206, y = 4.89360, \tau = 0.12276, d_2 = 0.552225, k = 16$ or $k = 19$. **a** Small k and **b** large k

Theorem 4.10 *Assume that* $\hat{\mathcal{R}}_2(0,\tau) > 1$, $\tau > 0$ *so that the semi-trivial equilibrium* $E_{s0} = (\bar{x}_{10}, \bar{x}_{20}, 0)$ *exists. Then it is locally asymptotically stable if*

$$\hat{\mathcal{R}}_2(0,\tau) < \frac{b_0\ (2\,b_1\,p + q\,b_0)}{2\,s_2\,s_3\,y\,p + q\,d_2 + q\,y\,s_2^2} \quad \textit{and} \quad \hat{\mathcal{R}}_2(0,\tau) \le e^2. \tag{80}$$

Proof The characteristic equation of system (6) at E_{s0} is

$$\begin{aligned} G(\lambda,\tau) := (\lambda + p)\left[\lambda + k\left(2\,b_0\,b_1\,e^{-a\,\bar{x}_{20}}\bar{x}_{20} + q\,\bar{x}_{10} - 2\,s_2\,s_3\,\bar{x}_{20}\,y\right)\right] \\ \left[\lambda + d_2 + y\,s_2^2 + e^{-a\,\bar{x}_{20}}\,e^{-p\,\tau}\,b_0^2(a\,\bar{x}_{20} - 1)\,e^{-\lambda\,\tau}\right], \end{aligned} \tag{81}$$

where $\bar{x}_{10}, \bar{x}_{20}$ are shown in (79). Equation (81) has two real eigenvalues

$$\lambda_1 = -p < 0, \quad \lambda_2 = -k\left(2\,b_0\,b_1\,e^{-a\,\bar{x}_{20}}\bar{x}_{20} + q\,\bar{x}_{10} - 2\,s_2\,s_3\,y\,\bar{x}_{20}\right). \tag{82}$$

From (82), one can easily verify that

$$\lambda_2 < 0 \quad \text{if} \quad \hat{\mathcal{R}}_2(0,\tau) < \frac{b_0\ (2\,b_1\,p + q\,b_0)}{2\,s_2\,s_3\,y\,p + q\,d_2 + q\,y\,s_2^2}. \tag{83}$$

All other eigenvalues of (81) are determined by the same equation as (55). The remaining part of the proof is the same as the proof in Theorem 4.7 and is thus omitted. □

Next, we numerically explore the model dynamics, hoping to gain some information and insights about the roles that anti-predator defense of adult prey plays in predator–prey interactions.

المنارة للاستشارات

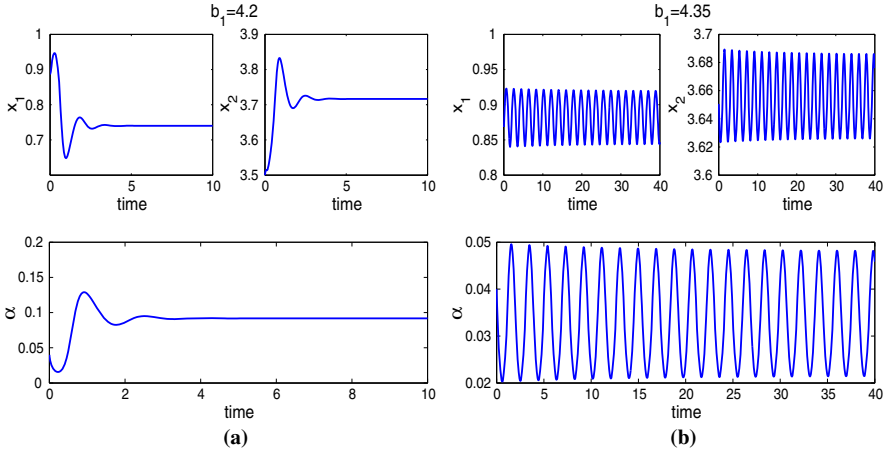

Fig. 14 Steady state or oscillation of system (6) with varying b_1. Parameters are: $b_0 = 3.07552, a = 0.38976, p = 0.750396, q = 0.2, s_2 = 0.562070, s_3 = 1.21206, y = 4.89360, \tau = 0.12276, d_2 = 0.552225, k = 18.31767, b_1 = 4.2$ or 4.35. **a** Small b_1 and **b** large b_1

We start by considering the impact of the parameter k which represents the sensitivity of adaptive anti-predator response. Figure 13a illustrates that, for relatively small k, the populations of both juvenile prey and adult prey, as well as the adaptive defense level of adult prey, all converge to positive constants. However, for relatively large k, we have observed periodic oscillations of the solutions of the model, as is shown in Fig. 13b. This indicates that, in addition to the maturation delay τ, this parameter of sensitivity may also destabilize an otherwise stable positive equilibrium, leading to the occurrence of periodic solutions.

Note that the parameter b_1 in the function $b(\alpha, x_2)$ describes how fast $b(\alpha, x_2)$ decreases with respect to the increase of α and hence accounts for the cost of the anti-predation response in the reproduction. The simulation results show that this parameter can also destabilize an otherwise stable positive equilibrium, as demonstrated in Fig. 14. Similar destabilizing effect by another parameter d_1, the cost of the fear in the death rate of the juveniles due to less sufficient care from the parental prey, has also been observed; see Fig. 15.

Our model assumes a simplest scenario for the predator population: constant predator population y (see the justification for this in the introduction). We now investigate the impact of this parameter. Interestingly, we have found that within certain range of other parameters, increasing y can stabilize an otherwise unstable positive equilibrium; see the simulation results in Fig. 16.

It is also interesting to examine the impact of key parameters on the components of a positive equilibrium. Figure 17 describes the dependence of E_{p1} on predator population y: Fig. 17a indicates that the population of both juvenile prey and adult prey decreases with increasing population of predators, and Fig. 17b shows that anti-predator defense level of adult prey increases with larger predator population—this is biologically reasonable (not surprising) because adult prey is easier to perceive predation risk with higher density of predators and demonstrates stronger anti-predator

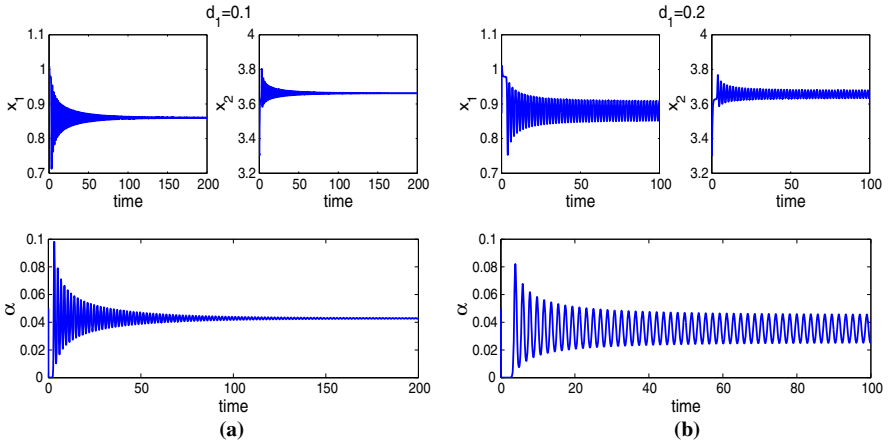

Fig. 15 Steady state or oscillation of system (6) with varying d_1. Parameters are: $b_0 = 3.07552, b_1 = 4.33876, a = 0.38976, p = 0.750396, s_2 = 0.562070, s_3 = 1.21206, \tau = 0.12276, d_2 = 0.552225, k = 18.31767, y = 4.8936, s_1 = 0.01, d_1 = 0.1$ or 0.2. **a** Small d_1 and **b** large d_1

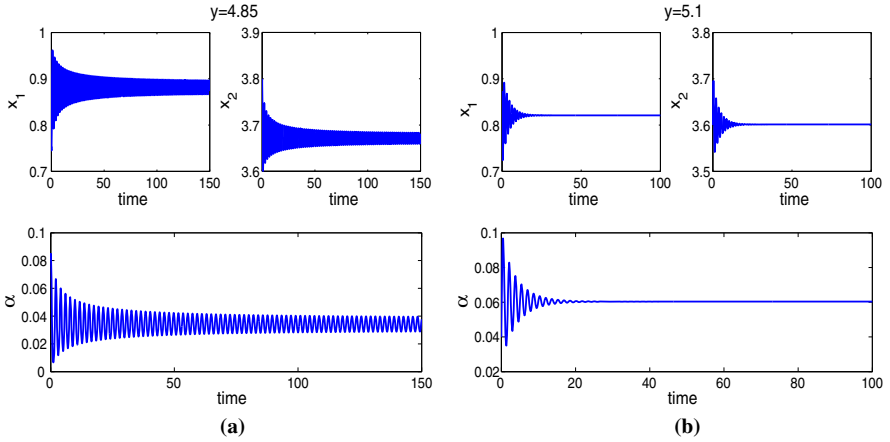

Fig. 16 Steady state or oscillation of system (6) with varying y. Parameters are: $b_0 = 3.07552, b_1 = 4.33876, a = 0.38976, p = 0.750396, q = 0.2, s_2 = 0.562070, s_3 = 1.21206, \tau = 0.12276, d_2 = 0.552225, k = 18.31767, y = 4.85$ or 5.1. **a** Small y, **b** large y

behaviors. Figure 18 shows the dependence of E_{p1} on the cost of fear b_1 in the reproduction while fixing other parameters. Figure 18a demonstrates that adult prey population decreases with increasing cost of fear. Figure 18b indicates that adult prey shows weaker anti-predator behaviors if the cost of such behaviors becomes too larger. Notice that from Fig. 18a, the population of juvenile increases slowly with large b_1. This is because adult prey devotes more energy in juvenile's reproduction and protection of juveniles with larger cost of anti-predator defense. As a consequence, the population of juvenile prey increases slightly.

المنارة للاستشارات

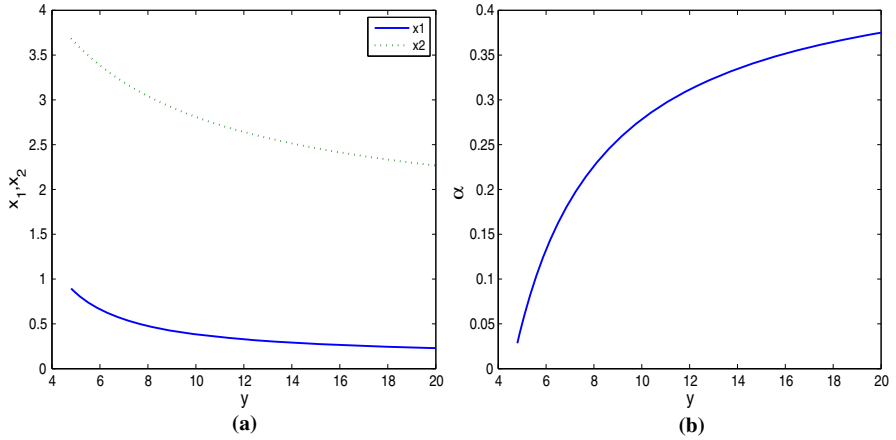

Fig. 17 Impact of y on the positive equilibrium $E_{p1}(\bar{x}_1, \bar{x}_2, \bar{\alpha})$. Parameters are: $b_0 = 3.07552, b_1 = 4.33876, a = 0.38976, p = 0.750396, q = 0.2, s_2 = 0.562070, s_3 = 1.21206, \tau = 0.12276, d_2 = 0.552225$. **a** Impact of y on $\bar{x}_1, \bar{x}_2$ and **b** impact of y on α

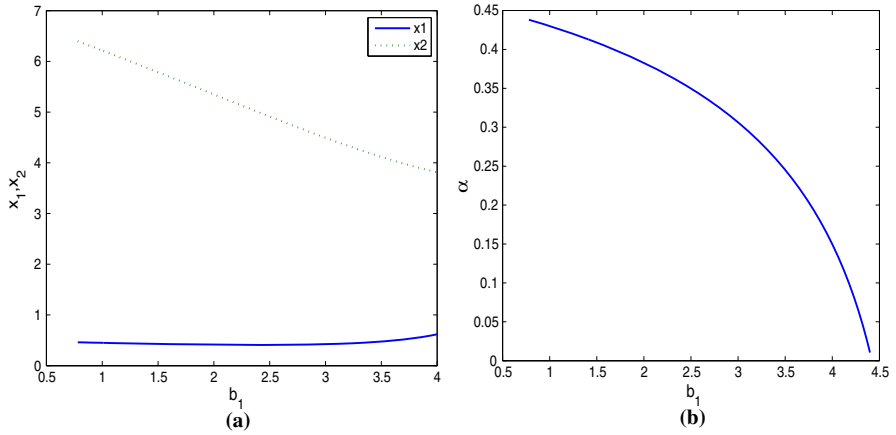

Fig. 18 Impact of b_1 on the positive equilibrium $E_{p1}(\bar{x}_1, \bar{x}_2, \bar{\alpha})$. Parameters are: $b_0 = 3.07552, a = 0.38976, p = 0.750396, q = 0.2, s_2 = 0.562070, s_3 = 1.21206, \tau = 0.12276, d_2 = 0.552225, y = 4.8936$. **a** Impact of b_1 on $\bar{x}_1, \bar{x}_2$ and **b** impact of b_1 on α

We also compare the effects that the adaptive defense level of adult prey α has on adult prey population with the case where α is a constant, i.e., the case when there is no adaptation for the strategy α. As shown in Fig. 19, the steady-state population of adult prey $\bar{x}_{21}$ in E_{p1} is always larger than the steady-state population of adult prey x_2^+ in (15) when $0 \leq \alpha \leq s_2/s_3$. Figure 19 indicates that adaptive defense of adults will have more benefit for prey in terms of its long-term population.

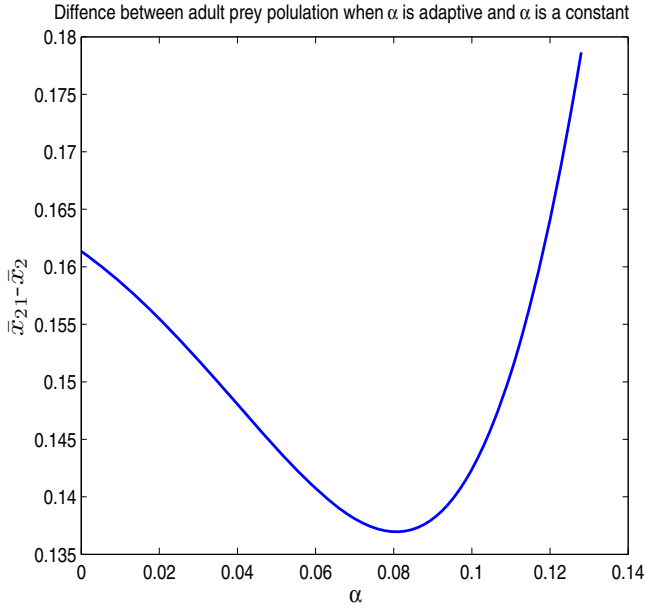

Fig. 19 Difference between $\bar{x}_{21}$ in $E_{p1}(\bar{x}_{21}, \bar{\alpha}_1)$ and x_2^+ in (15). Parameters are: $b_0 = 9.4609, b_1 = 13.2741, p = 0.0856, q = 3.0554, d_2 = 0.0467, s_2 = 0.2009, s_3 = 1.5685, y = 2.6194, \tau = 2.2335, a = 5$.

5 Conclusion and Discussion

Motivated by some recent experimental field study on the fear effect of prey, we proposed a mathematical model to examine the impact of the fear effect on the population dynamics of prey. The model is in the form of a system of delay differential equations. The novelty lies in the incorporation of *cost of the anti-predation response* of the prey both in the offspring reproduction (produce less) and the death of juveniles (high death rate due to less sufficient care from the parent prey), as well as the *adaptive* defense level. We have theoretically analyzed the model dynamics for two simpler cases and numerically explored the full model in the general case with focus on the impact that some key model parameters have on the long-term behaviors of solutions of the model.

Results show that, in addition to the maturation delay which has been found to destroy the stability of an equilibrium and cause periodic oscillations in many delay differential equation models, some other essential parameters can also affect the stability of an equilibrium, as illustrated in Sect. 4. While more rigorous and thorough analysis is still needed to obtain more qualitative and quantitative results about the full 3-d model, the numerical results based on the framework of the model have already provided some important information on the role that an anti-predator response may play in determining the long-term population dynamics. For example, in the case of a constant defense level, there may exist an optimal anti-predator defense level, and in the adaptive defense level case, within the certain ranges of parameters, periodic defense levels may be a choice. Most importantly, these results together with those recent field experimental results offered strong evidences of the significance of the

المنارة للاستشارات

fear effect in predator–prey interactions. All these seem to suggest the incorporation of the fear effect in existing predator–prey models, and consideration of such a new mechanism may lead to interesting and significant findings. For example, our recent work (Wang et al. 2016) on a simpler model with the fear effect offered an alternative way to eliminate the so-called paradox of enrichment.

In the model, the predator population is assumed to remain as a constant. Although there are numerous situations that fit in such a scenario, as we explained in the introduction, a case where the predator population is not a constant may intrigue further extensions. Here we outline how to modify the model (6) to accommodate nonconstant predator population. If the predator population varies with time, a fourth equation which describes the time evolution of predator population is obviously necessary. The equation for the adaptive defense level α still holds as it maximizes the instant growth rate of prey as a species, regardless of whether y remains a constant or not. From (6), it is clear that the population of predators y has an impact on prey's anti-predator defense level. For the case where y does not change with time, the impact that the predator population exerts on the avoidance behaviors of prey remains the same with evolution of time. However, prey selects anti-predator level depending on the current predator population and adjusts behaviors to instant change of the environment, if y is not a constant. However, in such a case, the corresponding model increases from three dimensions to four dimensions and is obviously very challenging and difficult to analyze. But we conjecture that a single optimal strategy for prey or periodic strategies for prey to avoid predation still exist if the predator population varies with time.

Another possible and important extension for future work is to incorporate the predation strategy for predators and study the coevolution with the avoidance strategy of prey. The coevolution is particularly important if the predator is a specialist predator because the ability to attack prey is essential for their own survival and reproduction. In such a scenario, both prey and predators adjust their behaviors depending on the current environment in order to gain the maximal benefits for each. It brings new framework for modeling and is thus interesting to analyze. However, due to the complexity and different focus of modeling, the stage structure of prey may no longer be a suitable choice because it obviously overcomplicates the potential model.

Furthermore, as far as the predator–prey interaction is concerned, spatial effect is an important factor due to foraging behaviors of both prey and predators. This suggests models with spatial dispersal, in addition to the spatial implicitly predation, anti-predator defense of prey, and the corresponding cost on prey population. All the aforementioned possible extensions are interesting, biologically important but yet mathematically challenging, and we have to leave them for future research projects.

Acknowledgements We benefitted a lot from the consultation and discussion with Dr. Liana Zanette in setting up the model, and we would like to thank Dr. Zanette for her friendly and generous help. We thank the two anonymous reviewers for their valuable suggestions and comments, which have led to a substantial improvement in the presentation of this paper.

References

Abrams PA (2000) The evolution of predator–prey interactions: theory and evidence. Annu Rev Ecol Syst 31:79–105

المنارة للاستشارات

Baer SM, Kooi BW, Kuznetsov YA, Thieme HR (2006) Multicodimensional bifurcation analysis of a basic two stage population model. SIAM J Appl Math 66:1339–1365
Beretta E, Kuang Y (2002) Geometric stability switch criteria in delay differential systems with delay dependent parameters. SIAM J Math Anal 33:1144–1165
Cooke KL, van den Driessche P, Zou X (1999) Interaction of maturation delay and nonlinear birth in population and epidemic models. J Math Biol 39:332–352
Cooke KL, Elderkin RH, Huang W (2006) Predator–prey interactions with delays due to juvenile maturation. SIAM J Appl Math 66:1050–1079
Creel S, Christianson D (2008) Relationships between direct predation and risk effects. Trends Ecol Evol 23:194–201
Creel S, Christianson D, Liley S, Winnie JA (2007) Predation risk affects reproductive physiology and demography of elk. Science 315:960–960
Cresswell W (2011) Predation in bird populations. J Ornithol 152:251–263
Faria T (2006) Asymptotic stability for delayed logistic type equations. Math Comput Model 43:433–445
Gourley SA, Kuang Y (2004) A stage structured predator–prey model and its dependence on maturation delay and death rate. J Math Biol 49:188–200
Győri I, Trofimchuk SI (2002) On the existence of rapidly oscillatory solutions in the Nicholson blowflies equation. Nonlinear Anal Theory Methods Appl 48:1033–1042
Křivan V (2007) The Lotka–Volterra predator–prey model with foraging–predation risk trade-offs. Am Nat 170:771–782
Kuang Y, So JW-H (1995) Analysis of a delayed two-stage population model with space-limited recruitment. SIAM J Appl Math 55:1675–1696
Lima SL (1998) Nonlethal effects in the ecology of predator–prey interactions. Bioscience 48:25–34
Lima SL (2009) Predators and the breeding bird: behavioural and reproductive flexibility under the risk of predation. Biol Rev 84:485–513
Liu S, Beretta E (2006) A stage-structured predator–prey model of Beddington–DeAngelis type. SIAM J Appl Math 66:1101–1129
Peacor SD, Peckarsky BL, Trussell GC, Vonesh JR (2013) Costs of predator-induced phenotypic plasticity: a graphical model for predicting the contribution of nonconsumptive and consumptive effects of predators on prey. Oecologia 171:1–10
Sheriff MJ, Krebs CJ, Boonstra R (2009) The sensitive hare: sublethal effects of predator stress on reproduction in snowshoe hares. J Anim Ecol 78:1249–1258
Svennungsen TO, Holen ØH, Leimar O (2011) Inducible defenses: continuous reaction norms or threshold traits? Am Nat 178:397–410
Shu H, Wang H, Wu J (2013) Global dynamics of Nicholson's blowflies equation revisited: onset and termination of nonlinear oscillations. J Differ Equ 255:2565–2586
Takeuchi Y, Wang W, Nakaoka S, Iwami S (2009) Dynamical adaptation of parental care. Bull Math Biol 71:931–951
Wang W, Nakaoka S, Takeuchi Y (2008) Invest conflicts of adult predators. J Theor Biol 253:12–23
Wang X, Zanette LY, Zou X (2016) Modelling the fear effect in predator–prey interactions. J Math Biol. doi:10.1007/s00285-016-0989-1
Wei J, Li M (2005) Hopf bifurcation analysis in a delayed Nicholson blowflies equation. Nonlinear Anal Theory Methods Appl 60:1351–1367
Wirsing AJ, Ripple WJ (2011) A comparison of shark and wolf research reveals similar behavioural responses by prey. Front Ecol Environ 9:335–341
Yamamichi M, Yoshida T, Sasaki A (2011) Comparing the effects of rapid evolution and phenotypic plasticity on predator–prey dynamics. Am Nat 178:287–304
Zanette LY, White AF, Allen MC, Clinchy M (2011) Perceived predation risk reduces the number of offspring songbirds produce per year. Science 334:1398–1401

المنارة للاستشارات

Reproduced with permission of copyright owner. Further reproduction prohibited without permission.

المنارة للاستشارات